DET NORSKE VERITAS

Final Report
Metallurgical Analysis of Leak on the 8-Inch Diameter Moosehorn Oil Pipeline

Pembina Pipeline Corporation
Calgary, Alberta

Report No./DNV Reg No.: ANEUS813GTQU (PP020915)
September 27, 2011

Metallurgical Analysis of Leak on 8-Inch Diameter Moosehorn Oil Pipeline	DET NORSKE VERITAS (U.S.A.), INC. Materials & Corrosion Technology Center 5777 Frantz Road Dublin, OH 43017-1386, United States Tel: (614) 761-1214 Fax: (614) 761-1633 http://www.dnv.com http://www.dnvusa.com
For: Pembina Pipeline Corporation 2000, 700-9 Avenue S.W. Calgary, Alberta T2P 3V4	
Account Ref.:	

Date of First Issue:	September 21, 2011	Project No.	PP020915
Report No.:		Organization Unit:	Materials & Corrosion Technology Ctr.
Revision No.:		Subject Group:	
Summary:			
Please see Executive Summary.			
Prepared by:	Greg T. Quickel, M.S. Senior Engineer	*Signature*	
Verified by:	John A. Beavers, Ph.D., FNACE Director – Failure Analysis	*Signature*	
Approved by:	Oliver C. Moghissi, Ph.D. Director, Materials & Corrosion Technology Center	*Signature*	Gerhardus H. Koch for Oliver C. Moghissi

☑	No distribution without permission from the client or responsible organizational unit (however, free distribution for internal use within DNV after 3 years)	Indexing Terms	
☐	No distribution without permission from the client or responsible organizational unit	Key Words	
☐	Strictly confidential	Service Area	
☐	Unrestricted distribution	Market Segment	

Rev. No. / Date:	Reason for Issue:	Prepared by:	Approved by:	Verified by

Executive Summary

Pembina Pipeline Corporation (*Pembina*) retained Det Norske Veritas (U.S.A.), Inc. (*DNV*) to perform a metallurgical analysis on a section of pipe from the 8-inch nominal diameter Deer Mountain Lateral crude oil pipeline that leaked in-service. The leak was discovered on July 19, 2011 in Swan Hills, Alberta at kilometer post (KP) 45.835, 7.73 m from the upstream (U/S) girth weld.

The portion of the pipeline that was removed is comprised 219.1 mm diameter by 4.8 mm wall thickness, API 5L X42 line pipe steel that contains an electric resistance welded (ERW) longitudinal seam. The maximum operating pressure (MOP) is 8275 kPa, which corresponds to 65.5% of the specified minimum yield strength (SMYS). The normal operating pressure is 5500 kPa, which corresponds to 43.5% of SMYS.

The pipeline was installed in 1961 and was externally coated with polyethylene tape and a fiberglass outer wrap. The coating at the leak was reportedly in fair to poor condition and contained liquid under the coating; the pH of a liquid sample was 6.5.

Following construction, a hydrostatic pressure test was performed. The pipeline has an impressed current cathodic protection (CP) system that was installed in 1961. Cathodic protection readings were taken on July 31, 2011 in the vicinity of the leak. Pipe to soil potentials were 1353 mV (on).

In the field, the coating had been removed, the pipe was cleaned, and magnetic particle inspection (MPI) was performed in the vicinity of the leak location. A 7.47 m section of pipe that contained the leak was shipped to DNV for analysis. The objectives of the analysis were to determine the metallurgical cause of the failure and identify any contributing factors.

The following steps were performed for this analysis. The pipe section was visually inspected and photographed. Wall thicknesses, diameters, and circumferences were measured on the pipe ends where coating was not present. Portions of the pipe that contained MPI indications were cleaned with a solvent. MPI was performed at these indications and the pipe was photographed. Pipe samples that contained the indications were removed from the pipe section, placed in liquid nitrogen, and hit with a hammer to reveal the fracture surfaces. The fracture surfaces were optically examined and photographed. The length and depths of the features on the fracture surfaces were measured to produce flaw profiles. Portions of the fracture surfaces were removed and cleaned with inhibited acid and a soft bristle brush. The cleaned fracture surfaces were examined in a scanning electron microscope (SEM) to document the fracture morphology and to determine if there was any evidence of in-service growth by fatigue. Axial and transverse cross-sections were removed from the mating fracture surfaces, mounted, polished, and etched.

Light photomicrographs were taken to document the feature morphologies and steel microstructure.

Mechanical testing (duplicate tensiles and full Charpy curve) was performed on transverse and axial, base metal and seam weld samples removed from the failed pipe joint. Chemical analysis was performed on a steel sample removed from the failed pipe joint to determine the composition.

The results of the analysis indicate that the leak occurred at a colony of circumferentially oriented, OD surface breaking, interlinked near-neutral-pH stress corrosion cracks that were located across the longitudinal seam weld (10:00 orientation). Supporting evidence for the conclusion that the cause of the rupture was near-neutral-pH SCC includes: (1) the presence of a colony of circumferentially oriented cracks on the external surface of the pipe in the vicinity of the failure origin; (2) the interlinking of individual thumbnail shaped cracks within the colony to form the initiating flaw; (3) the transgranular path of the cracks within the colony; (4) the presence of other crack colonies in the vicinity of the failure origin; and (5) evidence of corrosion of the crack faces.

Coincident with this colony were ID surface breaking circumferentially oriented cracks located at the seam weld; these cracks likely formed in the pipe mill from the trimming tool and are referred to as trimming cracks. The stress corrosion cracks propagated to one of these ID surface breaking cracks, producing the leak.

Below is a summary of our observations and conclusions.

- The leak occurred within a colony of OD surface breaking circumferentially oriented cracks.
- Other colonies were present on the pipe near the 3 and 9 o'clock orientations.
- The cracks within the colonies were characteristic of near-neutral-pH stress corrosion cracks.
- The pipe contained a slight bend and the intrados of the bend was located at the 6 o'clock orientation.
- The maximum depth of the stress corrosion crack at the leak site was 3.73 mm (78% of nominal wall thickness) deep. The through-wall length of the crack was 36 mm.
- The deepest stress corrosion crack identified on the pipe was 4.72 mm (98% of nominal wall thickness) in depth.

- A shallow axial hook crack was identified in the seam weld near a crack colony. The maximum depth of the hook crack was 0.226 mm (4.7% of nominal wall thickness).
- There was no evidence of fatigue crack growth of the stress corrosion cracks or hook crack.
- The mechanical properties of the pipe were better in the axial direction compared with transverse direction.
- The base metal tensile properties and chemical composition of the joint that failed meet specifications for API 5L X42 line pipe steel at the time of construction.
  - The average yield strength (YS) and ultimate tensile strength (UTS) for the duplicate transverse base metal samples were 331 MPa and 460 MPa, respectively.
  - The average YS and UTS for the duplicate axial base metal samples were 343 MPa and 467 MPa, respectively.
  - The average UTS of duplicate axial samples removed from the seam weld for the pipe section was 564 MPa.
  - Tensile test results for the transverse seam weld samples were not valid, but this test is not required for this vintage of API 5L.
  - The upper shelf Charpy energies (full size) for the transverse base metal, axial base metal, transverse seam weld, and axial seam weld samples were 46 J, 96 J, 37 J, and 103 J.
  - The Charpy energies (full size) for the transverse base metal, axial base metal, transverse seam weld, and axial seam weld samples tested at -4°C were 37.4 J, 75.8 J, 14 J, and 101 J.
- The microstructure of the pipe steel is consistent with the vintage and grade.

Several different regions were present on the fracture surfaces. Below is a summary of the regions:

- Region 1 (in all Colonies) – Transgranular, quasi-cleavage fracture (pre-existing, thumbnail shaped stress corrosion crack).
- Region 2 (in all Colonies) – Cleavage fracture from laboratory overload (brittle).
- Region 3 (in Colony 2 and 4) - Ductile fracture.

- Leak location, Colony 4 - Ductile shear cracking occurred on the inside pipe surface in the mill from the ERW trimming tool coincident with the leak location. Ductile fracture also occurred at the leak location, in-service.
- Colony 2 – A small ID surface breaking region, 2% of nominal wall thickness, was observed. It is not obvious when this ductile region formed.

- Region 4 (near Colony 5) – Relatively non-descript fractography, consistent with seam weld features (hook crack)
- Region 5 (near Colony 5) – Saw cut on one sample to facilitate breaking open of the fracture surface.

Table of Contents

List of Tables

List of Tables (continued)

List of Figures

List of Figures (continued)

List of Figures (continued)

List of Figures (continued)

List of Figures (continued)

1.0 BACKGROUND

Pembina Pipeline Corporation (*Pembina*) retained Det Norske Veritas (U.S.A.), Inc. (*DNV*) to perform a metallurgical analysis on a section of pipe from the 8-inch nominal diameter Deer Mountain Lateral crude oil pipeline that leaked in-service. The leak was discovered on July 19, 2011 in Swan Hills, Alberta at kilometer post (KP) 45.835, 7.73 m from the upstream (U/S) girth weld.

The portion of the pipeline that was removed is comprised 219.1 mm diameter by 4.8 mm wall thickness, API 5L X42 line pipe steel that contains an electric resistance welded (ERW) longitudinal seam. The maximum operating pressure (MOP) is 8275 kPa, which corresponds to 65.5% of the specified minimum yield strength (SMYS). The normal operating pressure is 5500 kPa, which corresponds to 43.5% of SMYS.

The pipeline was installed in 1961 and was externally coated with polyethylene tape and a fiberglass outer wrap. The coating at the leak was reportedly in fair to poor condition and contained liquid under the coating; the pH of a liquid sample was 6.5.

Following construction, a hydrostatic pressure test was performed. The pipeline has an impressed current cathodic protection (CP) system that was installed in 1961. Cathodic protection readings were taken on July 31, 2011 in the vicinity of the leak. Pipe to soil potentials were 1353 mV (on).

In the field, the coating had been removed, the pipe was cleaned, and magnetic particle inspection (MPI) was performed in the vicinity of the leak location. A 7.47 m section of pipe that contained the leak was shipped to DNV for analysis. The objectives of the analysis were to determine the metallurgical cause of the failure and identify any contributing factors.

2.0 TECHNICAL APPROACH

The procedures used in the analysis were in accordance with industry-accepted standards. Five of the general standards governing terminology, specific metallographic procedures, mechanical testing, and chemical analysis used are as follows:

- ASTM E7, “Standard Terminology Relating to Metallography.”
- ASTM E3, “Standard Methods of Preparation of Metallographic Specimens.”
- ASTM E8, “Test Methods for Tension Testing of Metallic Materials.”
- ASTM E23, “Standard Test Methods for Notched Bar Impact Testing of Metallic Materials.”

- ASTM A751, "Standard Test Methods, Practices, and Terminology for Chemical Analysis of Steel Products."

The following steps were performed for this analysis. The pipe section was visually inspected and photographed. Wall thicknesses, diameters, and circumferences were measured on the pipe ends where coating was not present. Portions of the pipe that contained MPI indications were cleaned with a solvent. MPI was performed at these indications and the pipe was photographed. Pipe samples that contained the indications were removed from the pipe section, placed in liquid nitrogen, and hit with a hammer to reveal the fracture surfaces. The fracture surfaces were optically examined and photographed. The length and depths of the features on the fracture surfaces were measured to produce flaw profiles. Portions of the fracture surfaces were removed and cleaned with inhibited acid and a soft bristle brush. The cleaned fracture surfaces were examined in a scanning electron microscope (SEM) to document the fracture morphology and to determine if there was any evidence of in-service growth by fatigue. Axial and transverse cross-sections were removed from the mating fracture surfaces, mounted, polished, and etched; see Figure 1 for the locations where samples were removed. Light photomicrographs were taken to document the feature morphologies and steel microstructure.

Mechanical testing (duplicate tensiles and full Charpy curve) was performed on transverse and axial, base metal and seam weld samples removed from the failed pipe joint. Chemical analysis was performed on a steel sample removed from the failed pipe joint to determine the composition; see Figure 1 for the locations where samples were removed.

3.0 RESULTS

3.1 Optical Examination

Figure 2 is a photograph of the pipe section as-received. The pipe section was wrapped in clear plastic and duct tape. The portion that leaked was also wrapped with electrical tape. The pipe section was approximately 7.47 m (24.5 feet) long and contained a longitudinal seam weld at the 10:00 orientation. Top-dead-center (TDC) and flow direction were marked on the pipe section.

Figure 3 is a photograph of the external pipe surface showing circumferential oriented crack colonies. The crack colony located at 7.73 m from the U/S girth weld (Colony 4) leaked; further discussion of the crack colonies is given in Section 3.2. The presence of white paint on the external pipe surface confirmed that MPI was performed in-the-field. It appeared MPI was performed on the majority of the external pipe surface.

Figure 4 is a photograph of the pipe section after removal of the protective wrappings. The figure shows that the pipe section contains a bend. The tape measure in the figure is located at the intrados of the bend. The maximum deflection is 23 mm, located at the 6 o'clock orientation, 8.946 m from the U/S girth weld.

The circumference, diameter, and wall thickness were measured at the U/S and downstream D/S pipe section ends. The diameters calculated from circumference measurements were 221 mm; see Table 1. The diameters were measured with a tape measure from the 3 to 9 o'clock and 12 to 6 o'clock orientations. The diameters at the ends were 219 mm, indicating no ovality. The diameter values are consistent with nominal 219.1 mm diameter pipe. The wall thickness was measured at the 12, 3, 6, and 9 o'clock orientations; see Table 2. The average wall thickness values for the U/S and D/S ends were 4.80 and 4.74 mm, respectively. These wall thickness values are consistent with the nominal wall thickness of 4.8 mm.

3.2 Magnetic Particle Inspection

Laboratory MPI of the external pipe surface was performed where crack colonies were identified in-the-field. Table 3 is a summary of the crack colony locations and dimensions. Six crack colonies were identified; Crack Colony 6 consisted of three sub colonies.

Figure 3 shows Crack Colonies 1, 2, and 4 prior to laboratory MPI; Figure 5 through Figure 8 are close-up photographs of the crack colonies. Crack Colonies 1, 2, and 4 were located about 7.5 m from the U/S girth weld, around the 9:00 o'clock orientation. Crack Colony 3 was located about 7.5 m from the U/S girth weld, around the 4:30 o'clock orientation. Crack Colonies 1 and 4 were the longest (in the circumferential direction) at 78 mm; the pipe leaked at Crack Colony 4.

Figure 9 shows Crack Colonies 5 and 6 prior to laboratory MPI; Figure 10 through Figure 13 are close-up photographs of the crack colonies. Crack Colonies 5 and 6 were located about 12.5 m from the U/S girth weld, around the 2:30 o'clock orientation. Crack Colony 5 was 55 mm in length and Crack Colony 6 was 60 mm in length.

3.3 Internal Surface

Figure 14 is a photograph of the internal pipe surface at the leak site, where Crack Colony 4 was located on the external pipe surface. The black dashed lines indicate the crack tips on the inside surface. The ID surface breaking portion of the crack is approximately 36 mm long. The figure shows some deformation around the crack, between and past the black dashed lines. Crack-like features are also located along the seam weld and are visible in the figure. These appear to have been formed in the mill during the trimming process. Figure 15 is a photograph of the internal pipe surface, where Crack Colony 2 is located on the external pipe surface. Some deformation is visible at this location. There does not appear to be any ID surface breaking cracks at this location.

3.4 Fracture Surface and Flaw Size Profile

Figure 16 is a photograph of the fracture surface after breaking open cracks at Colony 1. Two regions are identified on the fracture surface. Region 1 consists of multiple, OD surface

breaking, pre-existing thumbnail cracks with a black appearance. Region 2 consists of the remainder of the fracture surface and has a grey and shiny appearance. Region 2 is the overload region that occurred in the laboratory. The deepest portion of the crack was approximately 3.66 mm (76% of nominal wall thickness) deep.

Figure 17 is a photograph of the fracture surfaces after breaking open cracks at Colony 2. Regions 1 and 2 are indicated in the figure. Region 1 consists of OD surface breaking, pre-existing thumbnail cracks with a black appearance and Region 2 is the overload region that occurred in the laboratory. The deepest portion of the crack was approximately 4.72 mm (98% of nominal wall thickness) deep.

Figure 18 and Figure 19 are photographs of the fracture surfaces after breaking open cracks at Colony 4 (the leak location). Figure 19 shows the fracture surface after mild cleaning in Endox. Following cleaning, it is obvious that there are three regions on the fracture surface. Region 1 consists of OD surface breaking, pre-existing thumbnail cracks with a black appearance and Region 2 is the overload region that occurred in the laboratory. Region 3 has a dull, grey appearance, is located between the two regions at the crack ends, and is ID surface breaking near the middle of the thumbnail cracks. The morphology of Region 3 is not obvious at this magnification. The deepest portion of the thumbnail cracks was approximately 3.73 mm (78% of nominal wall thickness) deep.

Figure 20 is a photograph of the fracture surface after breaking open an axial feature near Colony 5. Three regions are indicated in the figure. Region 4 is an OD surface breaking, pre-existing shallow feature with a black appearance. Region 2 is the overload region that occurred in the laboratory. Region 5 is the saw cut that was made to facilitate breaking open of the shallow flaw. The deepest portion of the feature was approximately 0.226 mm (4.7% of nominal wall thickness) deep.

Figure 21 is a photograph of the fracture surface after breaking open a crack at Colony 6. Regions 1 and 2 are indicated in the figure. Region 1 consists of OD surface breaking, pre-existing thumbnail cracks with a black appearance and Region 2 is the overload region that occurred in the laboratory. The deepest portion of the crack was approximately 3.10 mm (65% of nominal wall thickness) deep.

Detailed crack length and depth measurements of the previously described thumbnail cracks and axial feature were taken to generate flaw profiles; see Figure 22 and Figure 23 for the graphs and Table 4 through Table 8 for length and depths. Figure 22 shows the flaws from the cracks and features removed from/near Colonies 1, 2, 5, and, 6. The figure shows that the thumbnail crack at Colony 2 was nearly through-wall. Figure 23 shows the flaws from the cracks removed

from Colony 4. The figure shows the depth of the pre-existing thumbnail shaped crack (Region 1) and the shows the flaw (Region 1+3) was through-wall.

3.5 Scanning Electron Microscopy

Figure 24 is an SEM image of fracture surface Sample S1 from Colony 1. The dashed line in the figure separates the pre-existing thumbnail crack (Region 1) from the overload region (Region 2). Figure 25 is a high magnification SEM image of the interface between Region 1 and 2. The fracture surface in Region 1 is corroded but contains some features consistent with quasi-cleavage. Quasi-cleavage is characteristic of near-neutral pH SCC. The figure also shows the cleavage facets that occurred in Region 2. The cleavage facets are consistent with brittle overload and formed during breaking open the sample in the laboratory. There was no evidence of fatigue striations near the interface between Region 1 and 2.

Figure 26 is an SEM image of fracture surface Sample S2 from Colony 2. The dashed line in the figure separates the pre-existing thumbnail crack (Region 1) from the overload regions (Region 2 and 3). Figure 27 is an SEM image showing the deepest portion of Region 1. The figure shows a smooth, semi-elliptical band in Region 1 above an overload region (Region 3). Figure 28 is a high magnification SEM image of the Region 1 just above this band (in Region 1). The fracture surface in Region 1 is corroded but contains features consistent with quasi-cleavage. Figure 29 is a high magnification SEM image of the fracture surface in the previously mentioned band. The figure shows pearlite grains and cleavage-like features, both that are consistent with transgranular fracture. This band in Region 1 may be a rapid fracture region that occurred in-service. Figure 30 is a SEM image in Region 3. The figures show a generally smeared morphology with some dimpled features. Dimples are consistent with ductile overload. This morphology was visible in the overload region between the vertical dashed lines in Figure 26. The morphology outside of the dashed lines in the overload region consisted of cleavage facets (Region 2, brittle overload) that occurred during breaking open the sample in the laboratory. It is not obvious when Region 3 (ductile overload) at this location on the pipe occurred.

Figure 31 is an SEM image of fracture surface Sample S4 from Colony 4 (leak location). The dashed line in the figure separates the pre-existing thumbnail crack (Region 1) from an overload region (Region 3). This portion of the overload region in the figure was located in the heat-affected zone (HAZ) of the seam weld. Figure 32 is an SEM image showing the interface of Region 1 and Region 3. Figure 33 is a high magnification SEM image of Region 1. The features are very corroded but contain some features that are consistent with quasi-cleavage. Figure 34 is a high magnification SEM image of the fracture surface in Region 3. The figures show ductile features with some smearing. The figure confirms that at ductile overload region (Region 3) was present at the leak location. The ductile region at this location likely occurred in the mill.

Figure 35 is a SEM image of Sample S4 near a crack tip. Regions 1 (thumbnail crack), 2 (brittle overload), and 3 (ductile overload) are indicated in the figure. Figure 36 is an SEM image at the interface of Regions 2 and 3. Region 3 consists of dimples and Region 2 consists of cleavage facets. Region 3 at this location likely occurred in-service. There was no evidence of fatigue crack growth on the fracture surface.

Figure 37 is an SEM image of fracture surface Sample S5a that was removed near Colony 5. The figure shows Region 4 and Region 2. Figure 38 is a high magnification SEM image of the interface between Region 4 and 2. Region 4 is relatively non-descript and there is no evidence of fatigue. Region 2 is the overload region that occurred in the laboratory.

Figure 39 is an SEM image of fracture surface Sample S6 from Colony 6. The dashed line in the figure separates the pre-existing thumbnail crack (Region 1) from the brittle overload region (Region 2). Figure 40 is a high magnification SEM image of Region 1 and 2. The fracture surface in Region 1 is corroded but contains features consistent with quasi-cleavage. Cleavage facets were identified in Region 2. There was no evidence of fatigue striations on the fracture surface.

3.6 Metallography

Figure 41 is a stereo light photomicrograph of axial metallographic section (Mount M1) that was removed from Crack Colony 1. OD surface breaking cracks are visible in the figure. The cracks are wider near the OD surface and thinner midwall. Figure 42 is a close-up light photomicrograph at the tip of a wider crack. The figure shows the thinner cracks; the crack path was transgranular. The presence of multiple pre-existing cracks is consistent with an SCC mechanism. The maximum depth of the cracks at this location was 3.26 mm (68% of nominal wall thickness).

Figure 43 is a stereo light photomicrograph of axial metallographic section (Mount M2) that was removed from Crack Colony 2. A broken open portion of the crack is shown in the middle of the mount. The maximum depth of the pre-existing thumbnail shaped crack was 98% of nominal wall thickness. OD surface breaking, secondary cracks are indicated in the figure. Figure 44 is light photomicrograph of the crack near the ID surface. The figure shows secondary cracks branching off of the primary crack. Figure 45 is a close-up light photomicrograph of Mount 2 near the ID surface. The dashed line indicates the interface between the Region 1 (thumbnail shaped crack) and 3 (ductile overload). Oxide is present on the crack face in Region 1. The grains are slightly deformed in Region 3, indicating that the overload was ductile. Figure 46 is a light photomicrograph of the typical microstructure of the base metal. The microstructure consists of ferrite (white areas), pearlite (gray areas consisting of lamellae), and inclusions (dark areas). This microstructure is consistent with the vintage and grade of the steel.

An axial metallographic cross-section (Mount M3) was removed from the pipe where Crack Colony 3 was reported to be located. No surface breaking features were identified.

Figure 47 is a stereo light photomicrograph of the axial metallographic section (Mount M4) that was removed from Crack Colony 4 at the initiation site. The trimming cracks (from the trimming tool), that were shown on the ID surface, are shown in cross-section. The darker appearance near the ID surface suggests that the material was work hardened. Figure 48 is a light photomicrograph of Mount M4. Branched, secondary cracks are visible near the OD surface. The crack face in Region 3 is approximately 45° relative to the free surface. An ID surface breaking crack at 135° relative to the free surface is also visible. These cracks at 45° and 135° are consistent with rerounding cracks that form from mechanical damage and gouges. These cracks were likely formed during the seam weld trimming process. Figure 49 is a close-up light photomicrograph showing the crack tip of the primary thumbnail crack (Region 1) and a portion of the rerounding crack (Region3). Oxide is located on the crack face in Region 1. The figure shows the morphology of the rerounding crack at the crack tip. Figure 50 is a close-up light photomicrograph of Mount M4 near the ID surface. The figure shows elongated grains. The elongated grains are from the trimming process. Figure 51 is a close-up light photomicrograph of a secondary crack tip. The figure shows that the crack path is transgranular, which is consistent with near neutral pH SCC.

Figure 52 is a stereo light photomicrograph of transverse metallographic section (Mount M5a), which was removed near Crack Colony 5. The altered microstructure associated with the ERW and the electrical contact marks on the OD pipe surface are evident in the cross section. There is no evidence of microstructural boundaries associated with a post weld heat treatment. These weld features are consistent with this vintage of ERW pipe, likely made by the low frequency (LF) process. Figure 53 is a light photomicrograph of Mount 5a. The figure shows a shallow, OD surface breaking hook crack located off of the bond line. The maximum depth of the crack at this location was 0.226 mm (4.7% of nominal wall thickness). Figure 54 is a close-up light photomicrograph at the crack tip. The figure shows a relatively wide tip. There is no evidence of fatigue of the hook crack.

Figure 55 and Figure 56 are light photomicrographs of the metallographic cross-sections (Mounts M5b and M6) removed from Crack Colonies 5b and 6. The figures show shallow, OD surface breaking cracks. The crack paths are transgranular. The maximum depth of the cracks at these locations for Mounts M5b and 6 were 0.258 mm (5.4% of nominal wall thickness) and 0.691 mm (14% of nominal wall thickness).

3.7 Mechanical Testing

The results of the base metal and seam weld tensile testing are shown in Table 9. The average yield strength (YS) and ultimate tensile strength (UTS) for the duplicate transverse base metal

samples were determined to be 331 MPa and 460 MPa, respectively. The average YS and UTS for the duplicate axial base metal samples were determined to be 343 MPa and 467 MPa, respectively. The YS and UTS for testing in both directions exceed the minimum YS and UTS specification for API 5L Grade X42 line pipe steel of 290 MPa, and 414 MPa, respectively, at the time of manufacture.

The average UTS of duplicate axial samples removed from the seam weld for the pipe section was 564 MPa, which exceeds the minimum specified value for API 5L Grade X42 line pipe steel of 414 MPa. YS values across the weld are not reliable and are not specified in API 5L. For the transverse seam weld samples, one of the samples broke during flattening and the other broke in a brittle manner at an ID feature. The UTS of the sample that failed at an ID feature was 242 MPa, which was below the minimum specified value for API 5L Grade X42 line pipe steel of 414 MPa.

Table 10 through Table 13 summarizes the results of the Charpy testing for the base metal and seam weld samples while Figure 57 through Figure 64 show the Charpy percent shear and impact energy curves. The Charpy energies (full size) for the transverse base metal, axial base metal, transverse seam weld, and axial seam weld samples tested at -4°C are 37.4 J, 75.8 J, 14 J, and 101 J. An analysis of the data for the transverse base metal indicates that the 85% fracture appearance transition temperature (FATT) is 22°C and the upper shelf Charpy energy is 46 J, full size. An analysis of the data for the axial base metal indicates that the 85% FATT is 4.4°C and the upper shelf Charpy energy is 96 J, full size. An analysis of the data for the transverse seam weld indicates that the 85% FATT is 66°C and the upper shelf Charpy energy is 37 J, full size. An analysis of the data for the axial seam weld indicates that the 85% FATT is -9.4°C and the upper shelf Charpy energy is 103 J, full size. The CVN test results can be adjusted to account for material constraint effects by applying temperature shifts to the data.[1] The full size transition temperatures (brittle-to-ductile fracture initiation temperature) for the transverse base metal, axial base metal, transverse seam weld, and axial seam weld samples were 50°C, 30°C, 104°C, and 21°C, respectively, based on a pipe wall thickness of 4.78 mm; see Table 14. The tested materials are expected to exhibit ductile fracture behavior above their full size transition temperatures.

3.8 Chemical Analysis

The results of the chemical analysis performed on a sample removed from the pipe joint that leaked is shown in Table 15. The results show that the pipe joint meets composition specifications for API 5L Grade X42 line pipe steel at the time of manufacture.

[1] "A Simple *Procedure* for Synthesizing Charpy Impact Energy Transition Curves from Limited Test Data," Michael J. Rosenfeld, International Pipeline Conference – Volume 1, ASME 1996, p. 216.

4.0 CONCLUSIONS

The results of the analysis indicate that the leak occurred at a colony of circumferentially oriented, OD surface breaking, interlinked near-neutral-pH stress corrosion cracks that were located across the longitudinal seam weld (10:00 orientation). Supporting evidence for the conclusion that the cause of the rupture was near-neutral-pH SCC includes: (1) the presence of a colony of circumferentially oriented cracks on the external surface of the pipe in the vicinity of the failure origin; (2) the interlinking of individual thumbnail shaped cracks within the colony to form the initiating flaw; (3) the transgranular path of the cracks within the colony; (4) the presence of other crack colonies in the vicinity of the failure origin; and (5) evidence of corrosion of the crack faces.

Coincident with this colony were ID surface breaking circumferentially oriented cracks located at the seam weld; these cracks likely formed in the pipe mill from the trimming tool and are referred to as trimming cracks. The stress corrosion cracks propagated to one of these ID surface breaking cracks, producing the leak.

Below is a summary of our observations and conclusions.

- The leak occurred within a colony of OD surface breaking circumferentially oriented cracks.
- Other colonies were present on the pipe near the 3 and 9 o'clock orientations.
- The cracks within the colonies were characteristic of near-neutral-pH stress corrosion cracks.
- The pipe contained a slight bend and the intrados of the bend was located at the 6 o'clock orientation.
- The maximum depth of the stress corrosion crack at the leak site was 3.73 mm (78% of nominal wall thickness) deep. The through-wall length of the crack was 36 mm.
- The deepest stress corrosion crack identified on the pipe was 4.72 mm (98% of nominal wall thickness) in depth.
- A shallow axial hook crack was identified in the seam weld near a crack colony. The maximum depth of the hook crack was 0.226 mm (4.7% of nominal wall thickness).
- There was no evidence of fatigue crack growth of the stress corrosion cracks or hook crack.

- The mechanical properties of the pipe were better in the axial direction compared with transverse direction.
- The base metal tensile properties and chemical composition of the joint that failed meet specifications for API 5L X42 line pipe steel at the time of construction.
  - The average yield strength (YS) and ultimate tensile strength (UTS) for the duplicate transverse base metal samples were 331 MPa and 460 MPa, respectively.
  - The average YS and UTS for the duplicate axial base metal samples were 343 MPa and 467 MPa, respectively.
  - The average UTS of duplicate axial samples removed from the seam weld for the pipe section was 564 MPa.
  - Tensile test results for the transverse seam weld samples were not valid, but this test is not required for this vintage of API 5L.
  - The upper shelf Charpy energies (full size) for the transverse base metal, axial base metal, transverse seam weld, and axial seam weld samples were 46 J, 96 J, 37 J, and 103 J.
  - The Charpy energies (full size) for the transverse base metal, axial base metal, transverse seam weld, and axial seam weld samples tested at -4°C were 37.4 J, 75.8 J, 14 J, and 101 J.
- The microstructure of the pipe steel is consistent with the vintage and grade.

Several different regions were present on the fracture surfaces. Below is a summary of the regions:

- Region 1 (in all Colonies) – Transgranular, quasi-cleavage fracture (pre-existing, thumbnail shaped stress corrosion crack).
- Region 2 (in all Colonies) – Cleavage fracture from laboratory overload (brittle).
- Region 3 (in Colony 2 and 4) - Ductile fracture.
  - Leak location, Colony 4 - Ductile shear cracking occurred on the inside pipe surface in the mill from the ERW trimming tool coincident with the leak location. Ductile fracture also occurred at the leak location, in-service.
  - Colony 2 – A small ID surface breaking region, 2% of nominal wall thickness, was observed. It is not obvious when this ductile region formed.

- Region 4 (near Colony 5) – Relatively non-descript fractography, consistent with seam weld features (hook crack)
- Region 5 (near Colony 5) – Saw cut on one sample to facilitate breaking open of the fracture surface.

Table 1. Results of circumference and diameter measurements performed on the U/S and D/S ends of the pipe section.

Pipe Section End	Circumference (mm)	Diameter from Circumference Measurement (mm)	Diameter 3 to 9 o'clock (mm)	Diameter 6 to 12 o'clock (mm)
U/S	692	221	219	219
D/S	692	221	219	219

Table 2. Results of wall thickness measurements performed on the U/S and D/S ends of the pipe section.

O'clock Orientations	Wall Thickness, U/S End (mm)	Wall Thickness, D/S End (mm)
12:00	4.80	4.72
3:00	4.80	4.72
6:00	4.83	4.70
9:00	4.75	4.83
Average	4.80	4.74

Table 3. Summary of the crack colony locations.

Crack Colony	Distances from Reference End (m)[1]	O'clock Orientation	Axial Length (mm)	Circumferential Length (mm)
1	7.47	9:44	82.6	78
2	7.55	8:38	44.5	52
3	7.70	4:22	-	18
4	7.73	9:52	82.6	78
5	12.36	2:14	55	55
6	12.51	2:24	160	60
6A [2]	12.60	2:28	15	35
6B [2]	12.61	2:14	55	45
6C [2]	12.51	2:14	75	35

1. Distance from U/S end of colony.
2. Sub colonies of Crack Colony 2.

Table 4. Flaw profile (length vs. depth) for the pre-existing thumbnail shaped crack located on the fracture surface removed from Crack Colony 1.

Length (mm)	Depth	
	mm	% of nominal wall thickness
0	0	0
6.4	3.66	77
12.7	3.02	63
19.1	0	0

Table 5. Flaw profile (length vs. depth) for the pre-existing thumbnail shaped crack located on the fracture surface removed from Crack Colony 2.

Length (mm)	Depth	
	mm	% of nominal wall thickness
0	0	
6.35	2.62	55
12.7	4.04	85
19.1	4.72	99
25.4	2.69	56
31.8	4.22	88
38.1	3.91	82
44.5	2.11	44
49.3	0	0

Table 6. Flaw profile (length vs. depth) for the pre-existing thumbnail shaped crack (Region 1) and Region 1+3 located on the fracture surface removed from Crack Colony 4.

Length (mm)	Depth of Region 1		Depth of Region 1+3	
	mm	% of nominal wall thickness	mm	% of nominal wall thickness
0	0		0	0
6.35	1.75	37	2.72	57
12.7	1.17	24	3.31	69
19.1	2.36	49	4.78	100
25.4	2.06	43	4.78	100
31.8	1.96	41	4.78	100
38.1	3.05	64	4.78	100
44.5	3.73	78	4.78	100
50.8	3.05	64	4.78	100
57.2	1.52	32	2.77	58
63.5	0	0	0	0

Table 7. Flaw profile (length vs. depth) for the axial feature located on the fracture surface removed near Crack Colony 5.

Length (mm)	Depth	
	mm	% of nominal wall thickness
0	0.089	1.9
6.35	0.226	4.7
12.7	0.226	4.7
19.1	0.226	4.7
22.2	0	0

Table 8. Flaw profile (length vs. depth) for the pre-existing thumbnail shaped crack located on the fracture surface removed from Crack Colony 6.

Length (mm)	Depth	
	mm	% of nominal wall thickness
0	0	0
6.35	1.68	35
12.7	2.77	58
16.0	3.10	65
19.1	2.46	51
25.4	0	0

Table 9. Results of base metal and seam weld tensile tests performed on transverse and axial samples from the failed joint compared with specifications for API 5L Grade X42 line pipe steel.

	Transverse Base Metal	Axial Base Metal	Transverse Seam Weld	Axial Seam Weld	API 5L Grade X42 (Minimum Values) [2]
Yield Strength, MPa [1]	331	343	–	-	290
Tensile Strength, MPa [1]	460	467	242 [3]	564	414
Elongation in 2 inches, %	33.0	34.0	–	-	20.0
Reduction of Area, % [1]	51.0	55.0	–	-	–

1 – Average of duplicate tests.

2 – API Spec 5LX, 9th Edition, February 1960.

3 – One sample, failed in a brittle manner at an ID flaw. The other sample broke during flattening.

Table 10. Results of Charpy V-notch impact tests for transverse base metal samples removed from the failed pipe joint.

Sample ID	Temperature, °C	Sub-Size Impact Energy, J	Full Size Impact Energy, J	Shear, %	Lateral Expansion, mm
1	-59	2.7	7.3	0	0
2	-32	4.1	11	0	0
3	-18	12	33.2	30	0.25
4	-4	13.6	37.4	50	0.33
5	10	16.3	44.2	70	0.51
6	24	16.3	44.2	80	0.53
7	38	16.9	46.4	100	0.58
8	66	16.3	44.2	100	0.64
9	79	17.6	47.6	100	0.66
10	93	17.6	47.9	100	0.64

Table 11. Results of Charpy V-notch impact tests for axial base metal samples removed from the failed pipe joint.

Sample ID	Temperature, °C	Sub-Size Impact Energy, J	Full Size Impact Energy, J	Shear, %	Lateral Expansion, mm
1	-101	2.0	5.2	0	0
2	-32	12	31	10	0.38
3	-18	24.4	61.7	50	0.91
4	-4	29.8	75.8	75	1.1
5	10	31.2	79.3	85	1.1
6	24	35.3	89.6	90	1.2
7	38	35.3	90.2	98	1.2
8	52	38.0	96.5	100	1.4
9	66	39.3	101	100	1.2
10	79	38.0	96.5	100	1.2

Table 12. Results of Charpy V-notch impact tests for transverse seam weld samples removed from the failed pipe joint.

Sample ID	Temperature, °C	Sub-Size Impact Energy, J	Full Size Impact Energy, J	Shear, %	Lateral Expansion, mm
1	-4	4.1	14	0	0.05
2	10	5.4	19	15	0.10
3	24	5.4	19	30	0.23
4	38	4.7	16	25	0.15
5	52	6.1	20	65	0.25
6	66	6.8	23	90	0.33
7	79	12	42	100	0.53
8	93	9.5	33	100	0.38
9	107	12	41	100	0.43
10	135	9.5	33	100	0.46

Table 13. Results of Charpy V-notch impact tests for axial seam weld samples removed from the failed pipe joint.

Sample ID	Temperature, °C	Sub-Size Impact Energy, J	Full Size Impact Energy, J	Shear, %	Lateral Expansion, mm
1	-101	12	37	0	0.10
2	-59	17.6	49.2	15	0.25
3	-46	23.0	60.6	35	0.64
4	-32	24.4	64.1	40	0.64
5	-18	29.8	86.4	75	0.71
6	-4	35.3	101	98	1.2
7	10	36.6	102	100	0.94
8	24	37.3	111	100	1.0
9	38	35.3	97.8	100	0.89
10	52	32.5	97.1	100	0.79

Table 14. Results of analysis of the Charpy V-notch impact energy and percent shear plots for base metal and seam weld samples removed from the failed pipe joint.

	Transverse Base Metal	Axial Base Metal	Transverse Seam Weld	Axial Seam Weld
Upper Shelf Impact Energy (Full Size), J	46	96	37	103
85% FATT, °C	22	4.4	66	-9.4
85% FATT, °C (Full Size)	50	30	104	21

Table 15. Results of chemical analysis of a sample removed from the failed pipe joint compared with composition specifications (ladle analysis) for API 5L X42 line pipe steel.

Element		Composition (Wt. %)	API 5L X42 spec (Wt. %) [1]
C	(Carbon)	0.237	0.28 (max)
Mn	(Manganese)	0.861	1.25 (max)
P	(Phosphorus)	0.010	0.04 (max)
S	(Sulfur)	0.024	0.05 (max)
Si	(Silicon)	0.081	–
Cu	(Copper)	0.095	–
Sn	(Tin)	0.008	–
Ni	(Nickel)	0.036	–
Cr	(Chromium)	0.029	–
Mo	(Molybdenum)	0.006	–
Al	(Aluminum)	0.001	–
V	(Vanadium)	0.000	–
Nb	(Niobium)	0.001	–
Zr	(Zirconium)	0.000	–
Ti	(Titanium)	0.001	-
B	(Boron)	0.0001	–
Ca	(Calcium)	0.0000	–
Co	(Cobalt)	0.005	–
Fe	(Iron)	Balance	Balance

1 – API Spec 5LX, 9th Edition, February 1960, welded, electric-furnace, open-hearth, basic-oxygen or killed deoxidized basic Bessemer, cold-expanded.

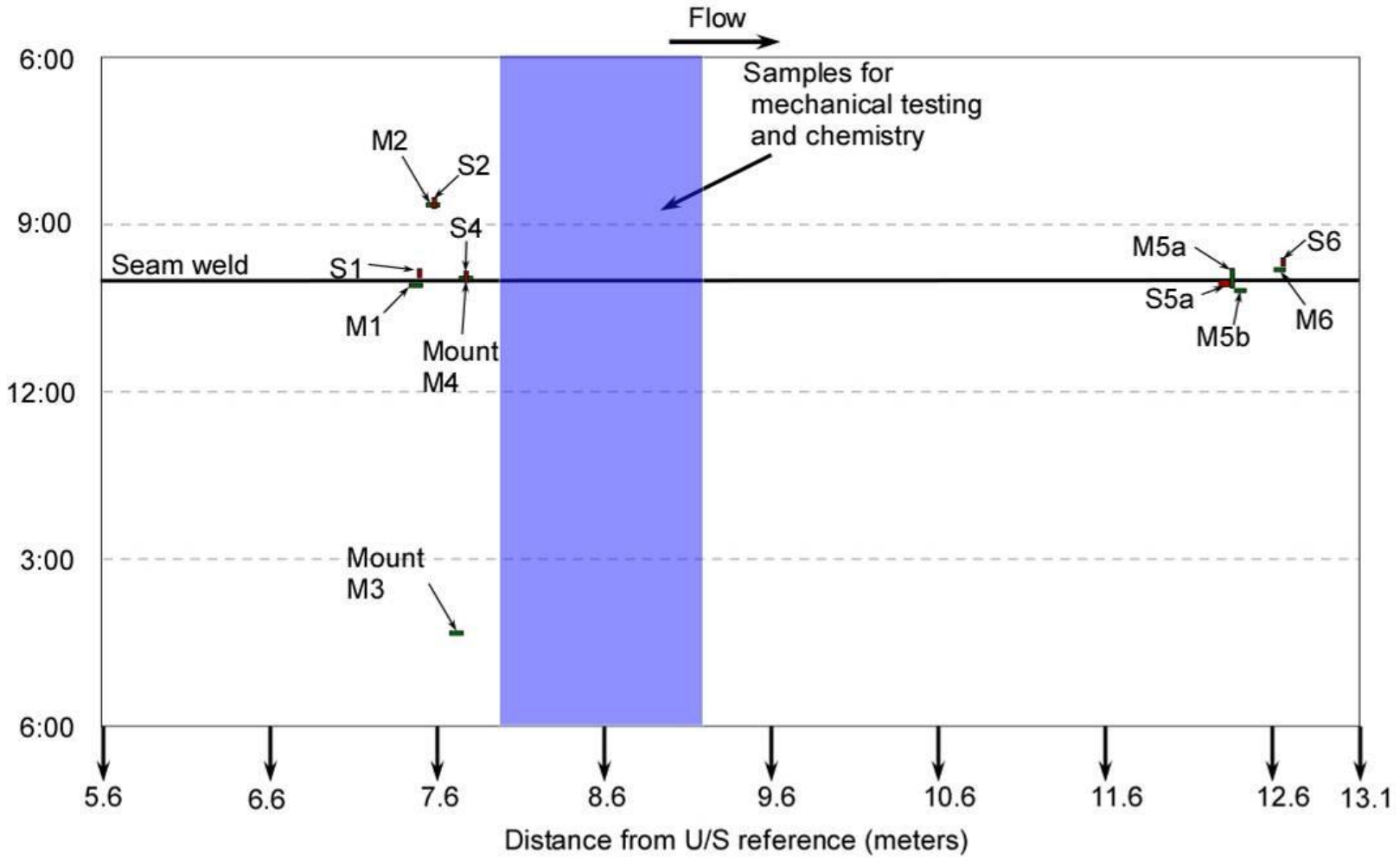

Figure 1. Schematic of pipe section showing the location of the seam weld and the locations where samples were removed for metallography (M1, 2, 3, 4, 5a, 5b, 6), fractography (S1, 2, 4, 5a, 6), mechanical testing, and chemistry.

Figure 2. Photograph of the pipe section in the as-received condition.

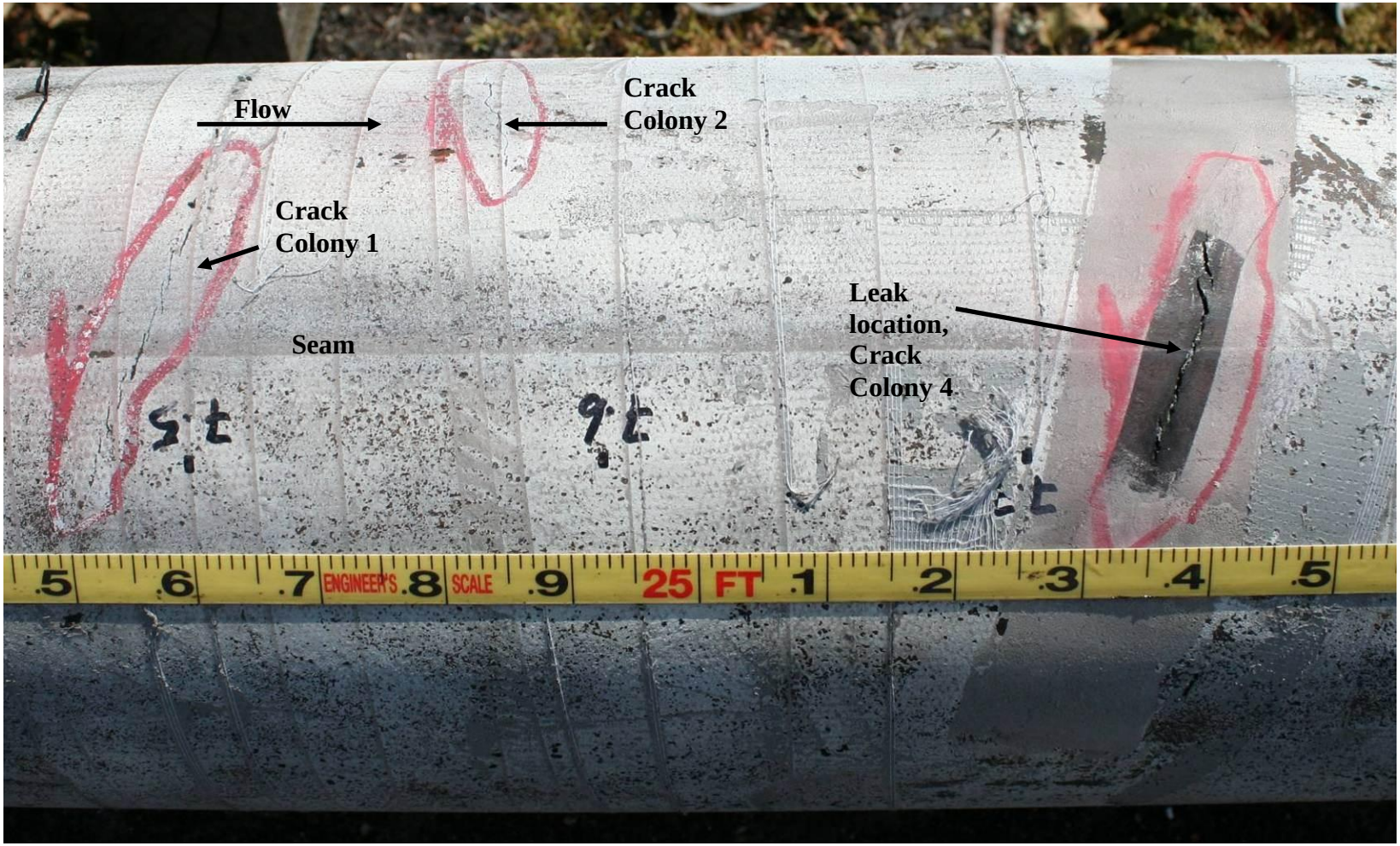

Figure 3. Photograph of the external pipe surface (prior to laboratory MPI) showing the leak location and crack colonies. The tape measure indicates the distance from the U/S girth weld.

Intrados of bend; maximum deflection approximately 23 mm at 8.946 m from the U/S girth weld

Figure 4. Photograph of the pipe section showing the bend.

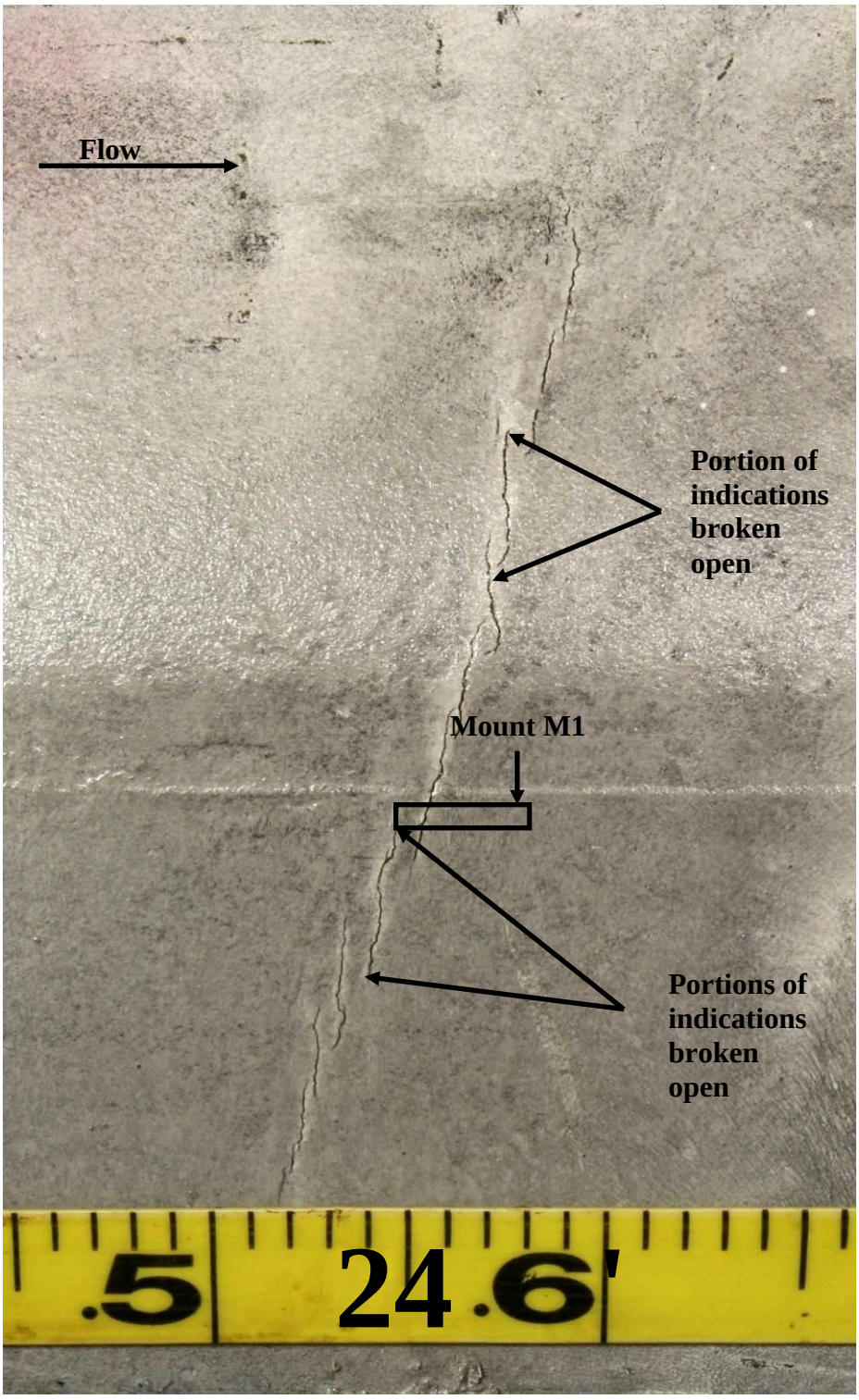

Figure 5. Photograph of the external pipe surface showing Crack Colony 1 following MPI. The tape measure indicates the distance from the U/S girth weld.

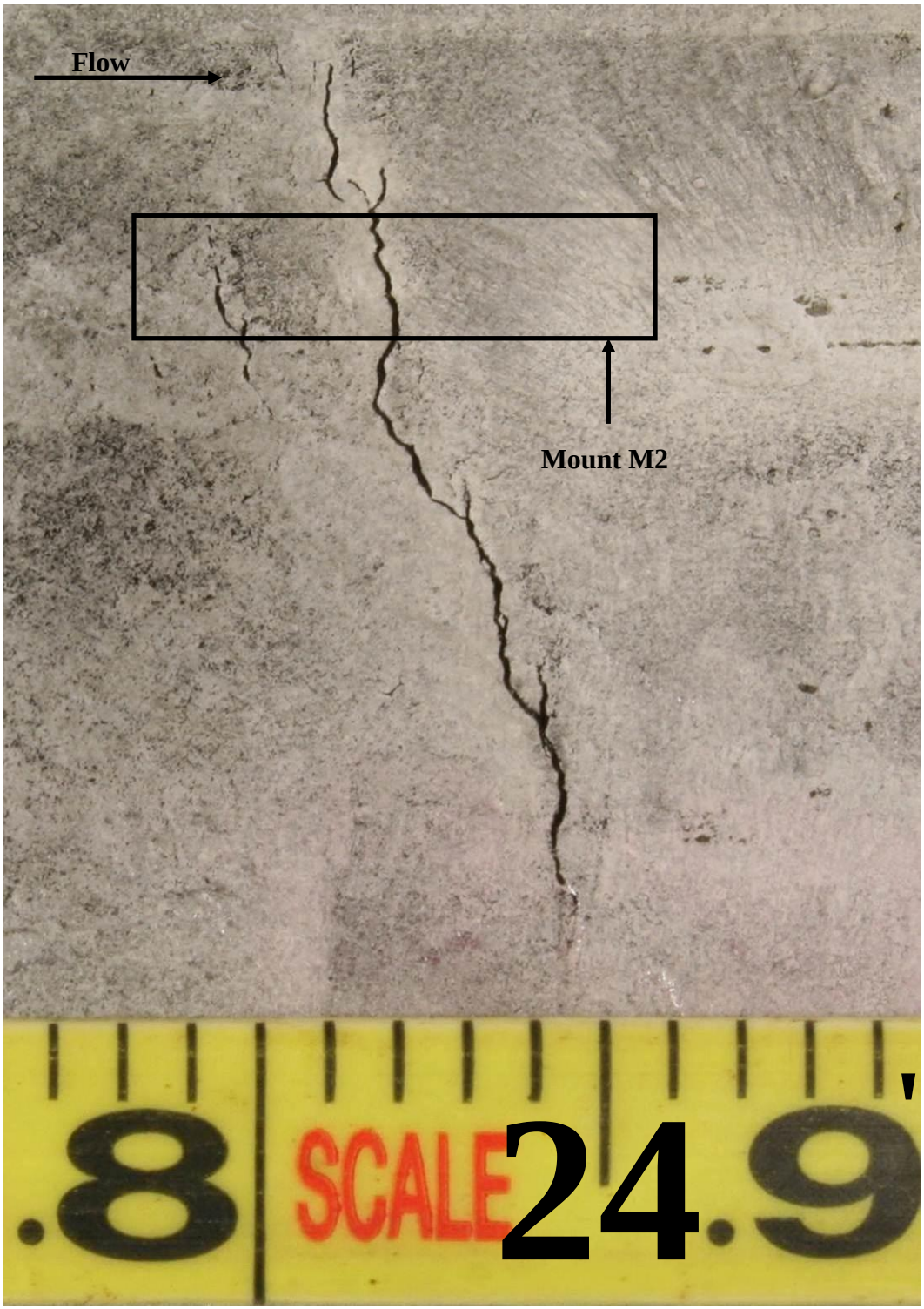

Figure 6. Photograph of the external pipe surface showing Crack Colony 2 following MPI. The tape measure indicates the distance from the U/S girth weld.

Figure 7. Photograph of the external pipe surface showing Crack Colony 3 following MPI. The tape measure indicates the distance from the U/S girth weld.

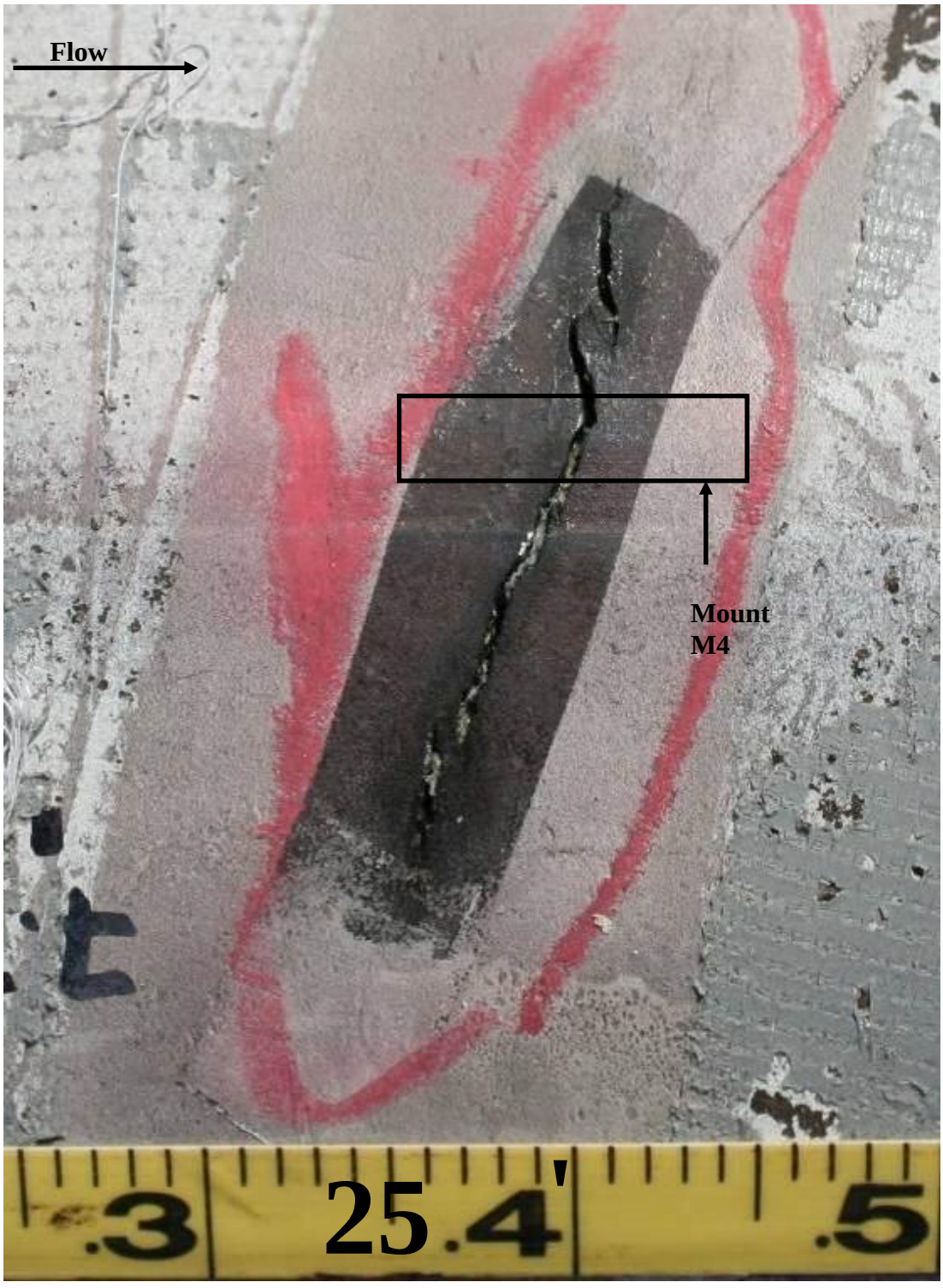

Figure 8. Photograph of the external pipe surface showing Crack Colony 4 (leak location), following MPI. The tape measure indicates the distance from the U/S girth weld.

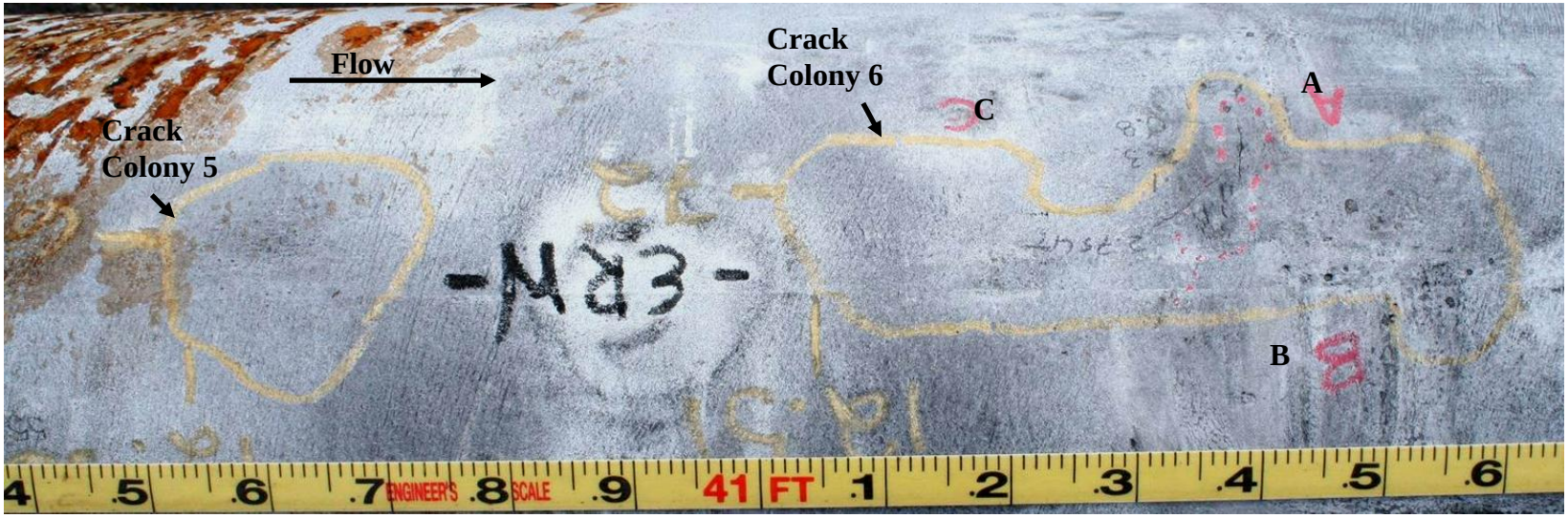

Figure 9. Photograph of the external pipe surface (prior to laboratory MPI) showing the crack colonies. The tape measure indicates the distance from the U/S girth weld.

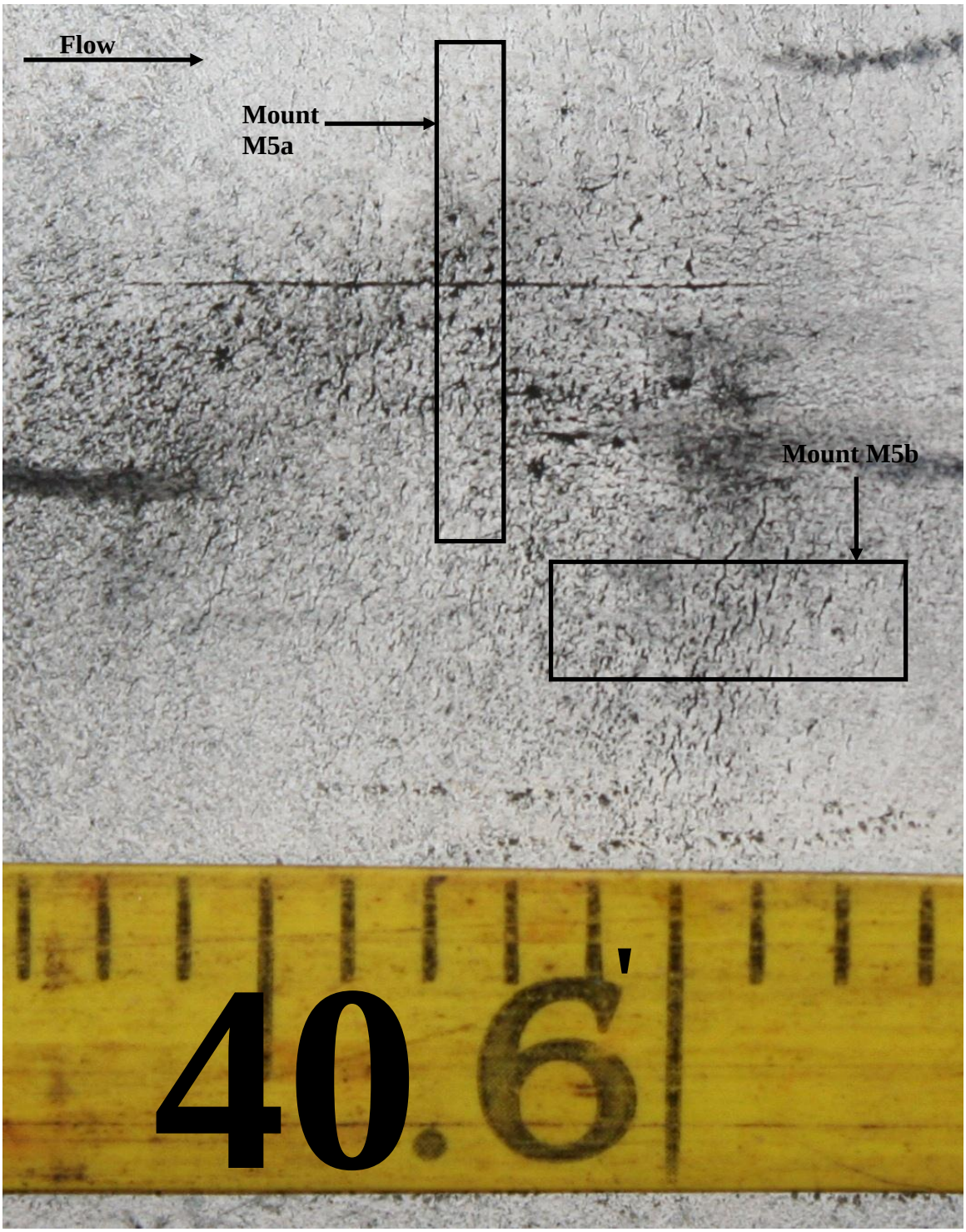

Figure 10. Photograph of the external pipe surface showing Crack Colony 5 following MPI. The tape measure indicates the distance from the U/S girth weld.

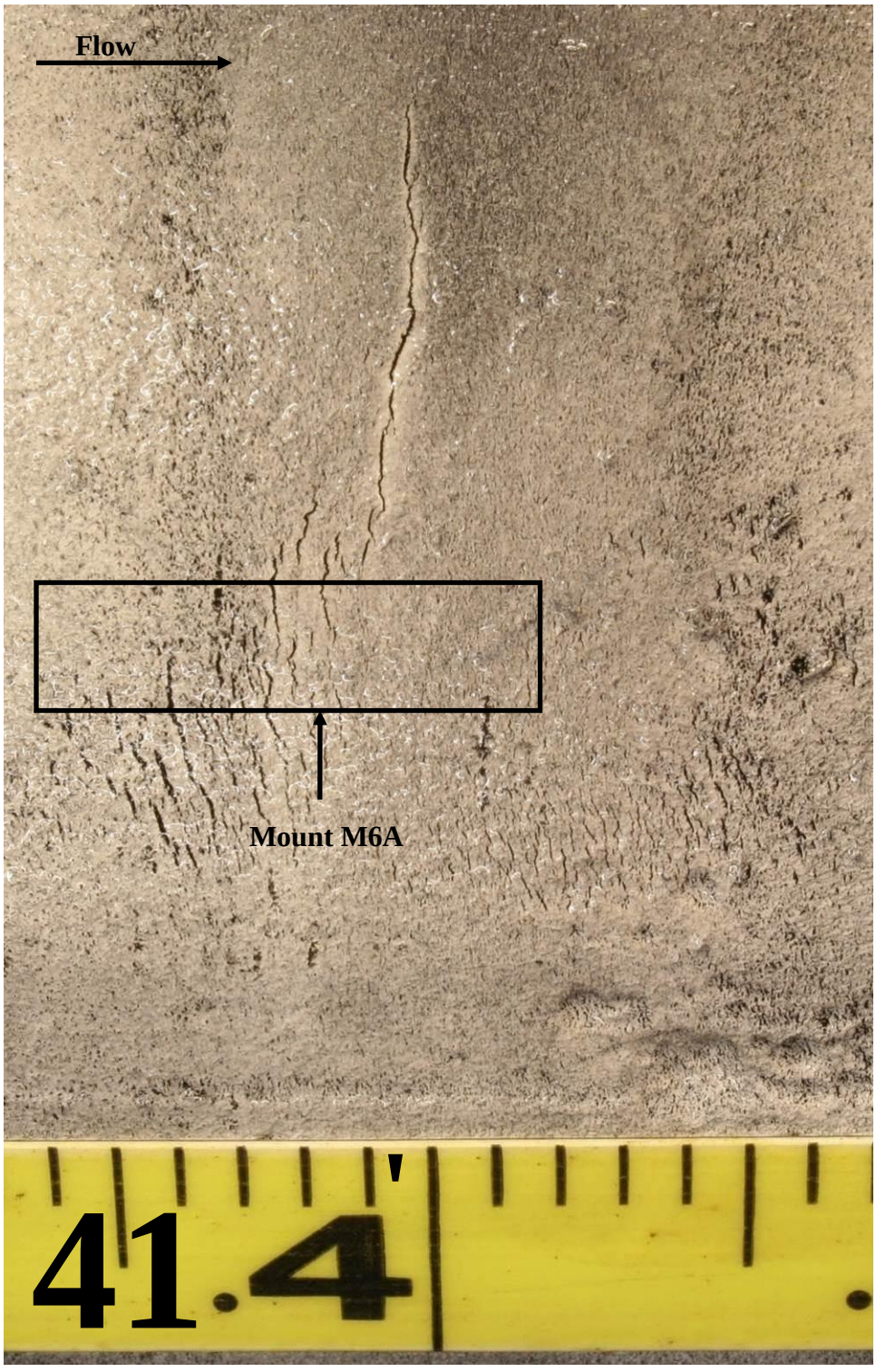

Figure 11. Photograph of the external pipe surface showing Crack Colony 6A following MPI. The tape measure indicates the distance from the U/S girth weld.

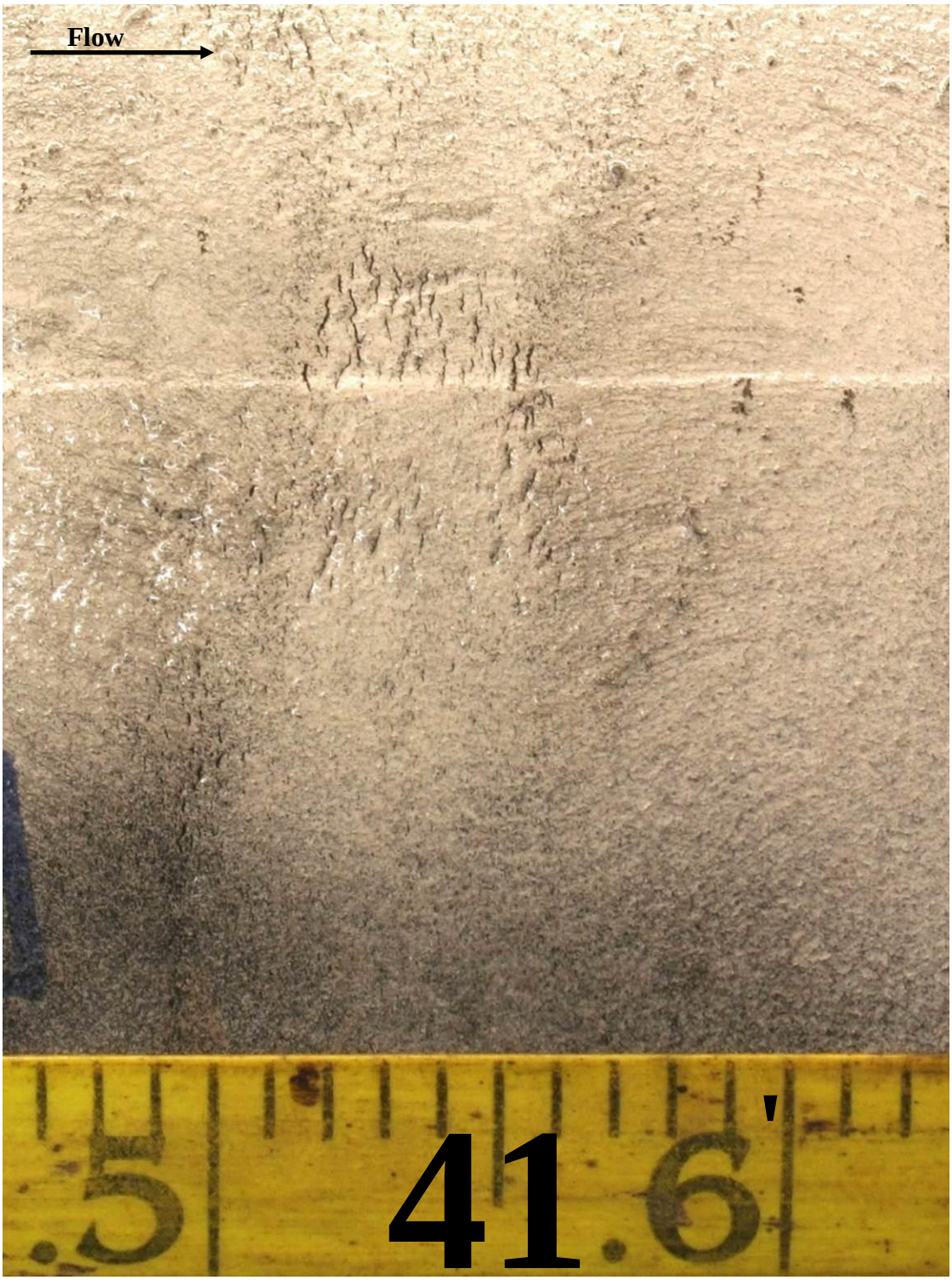

Figure 12. Photograph of the external pipe surface showing Crack Colony 6B following MPI. The tape measure indicates the distance from the U/S girth weld.

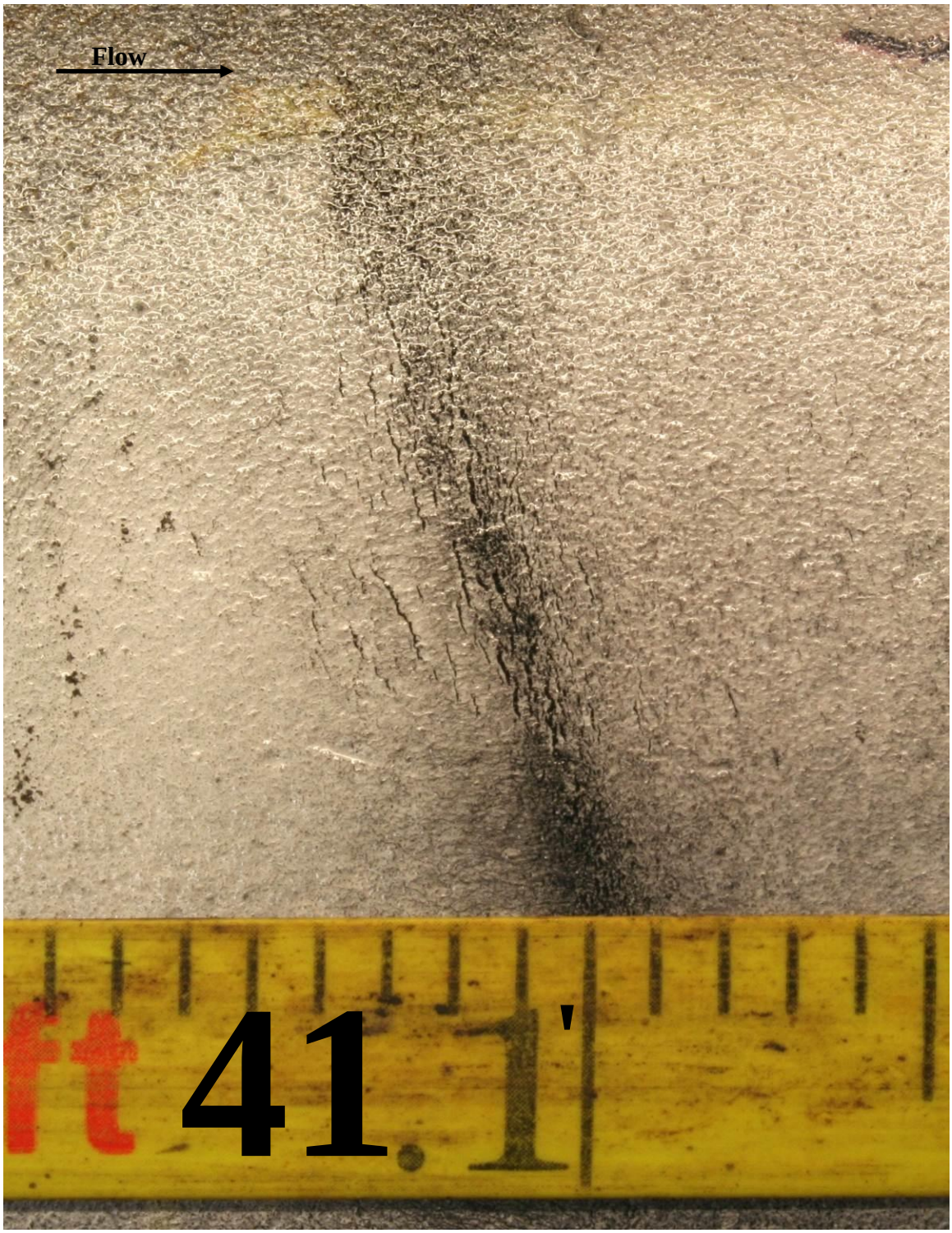

Figure 13. Photograph of the external pipe surface showing Crack Colony 6C following MPI. The tape measure indicates the distance from the U/S girth weld.

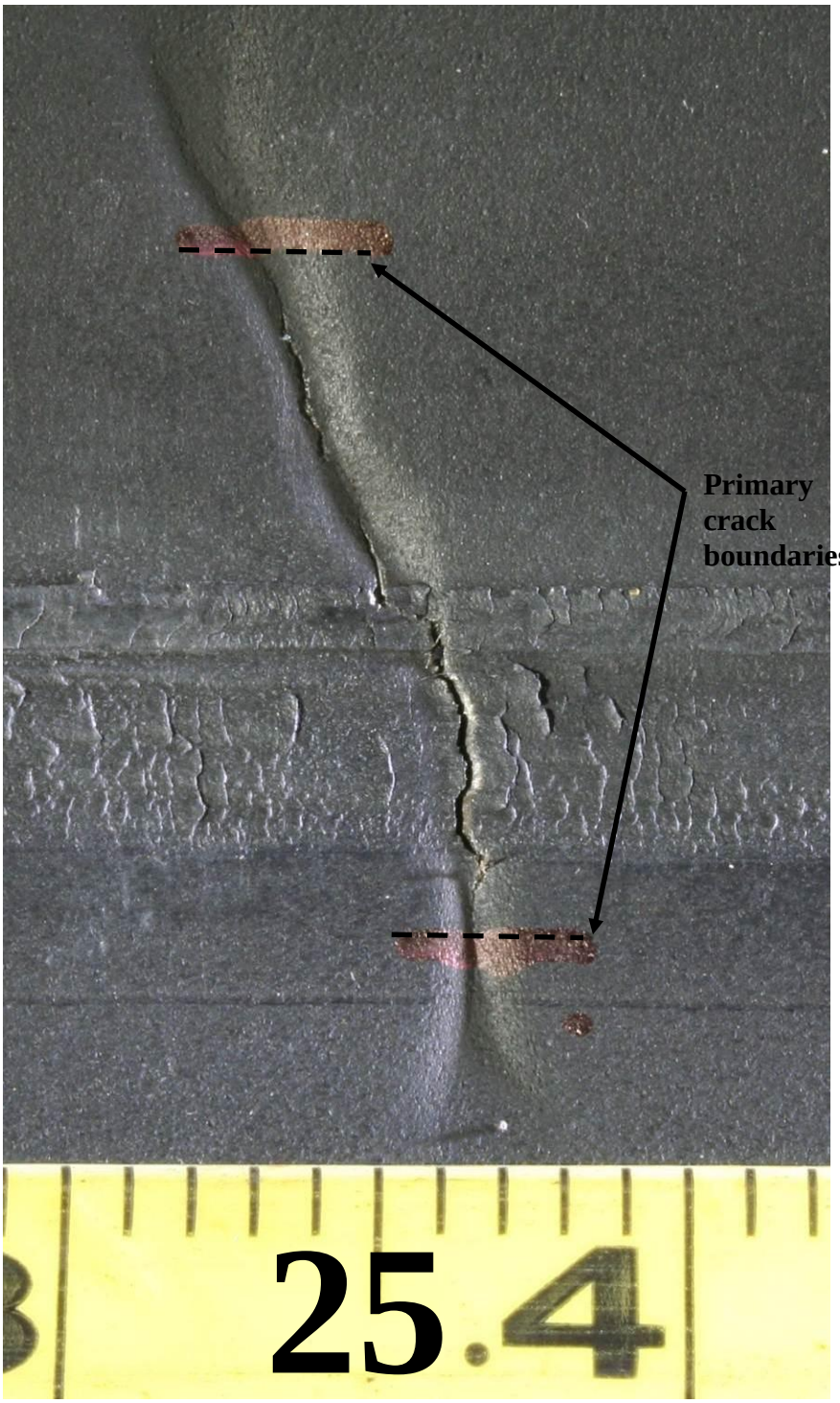

Figure 14. Photograph of the internal pipe surface at the leak location (Crack Colony 4). The tape measure indicates the distance from the U/S girth weld.

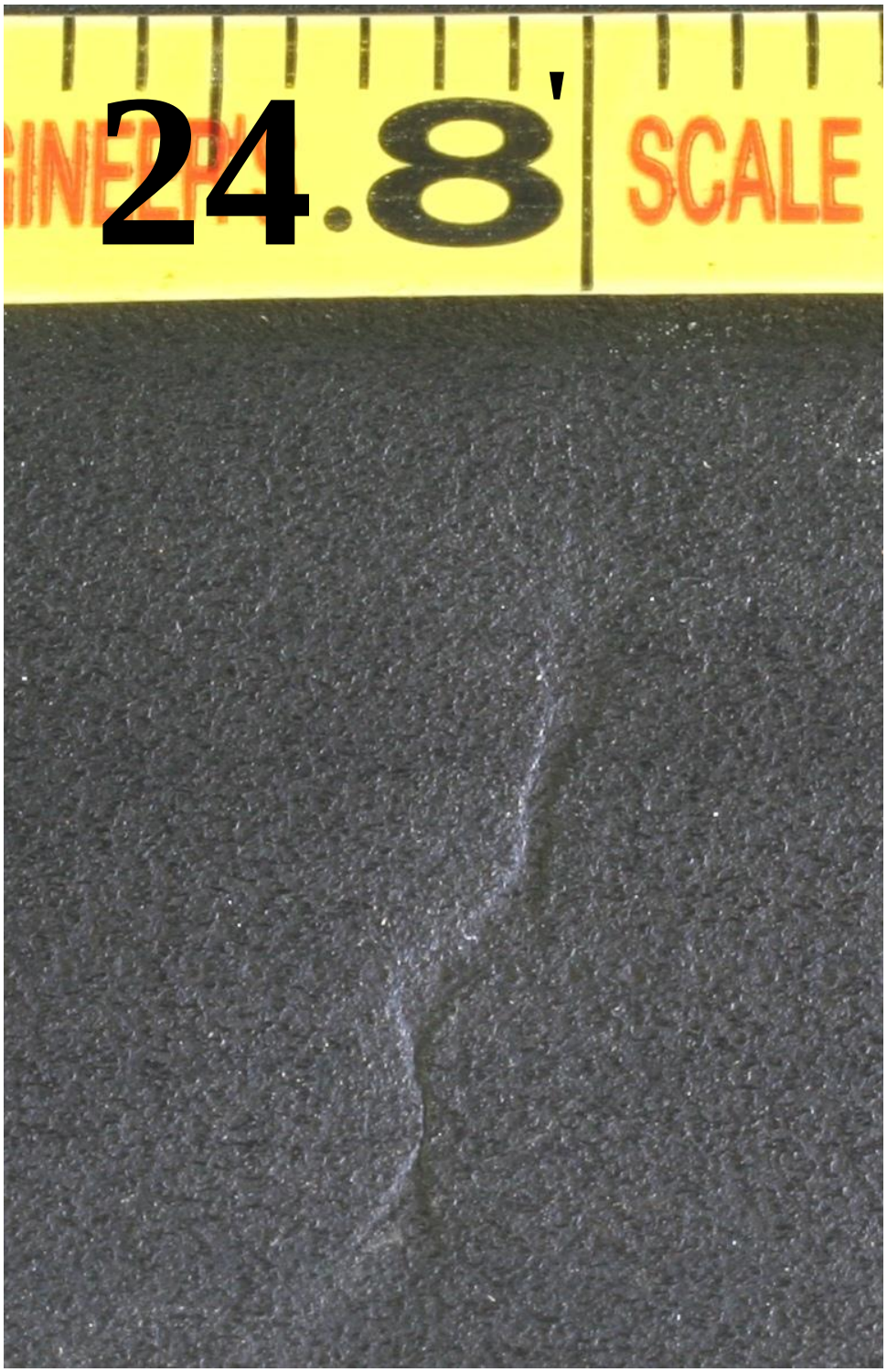

Figure 15. Photograph of the internal pipe surface at the location of Crack Colony 2. The tape measure indicates the distance from the U/S girth weld.

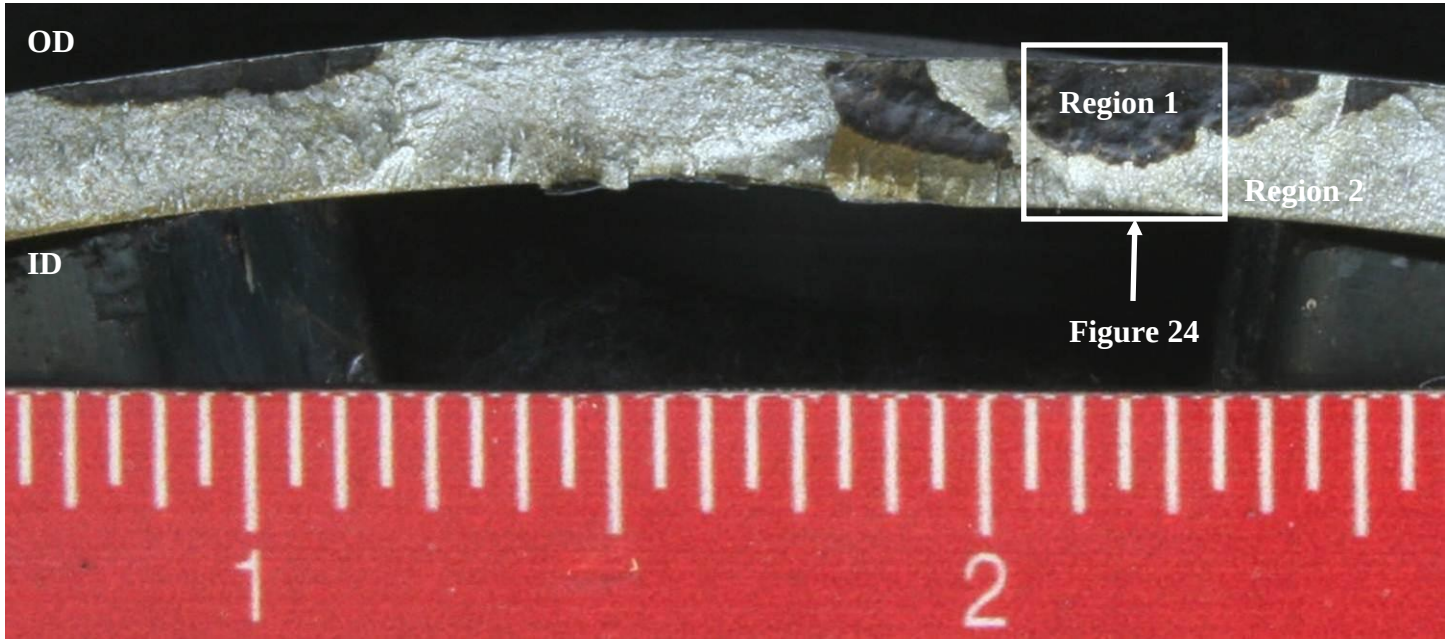

Figure 16. Photograph of the fracture surface removed from Crack Colony 1.

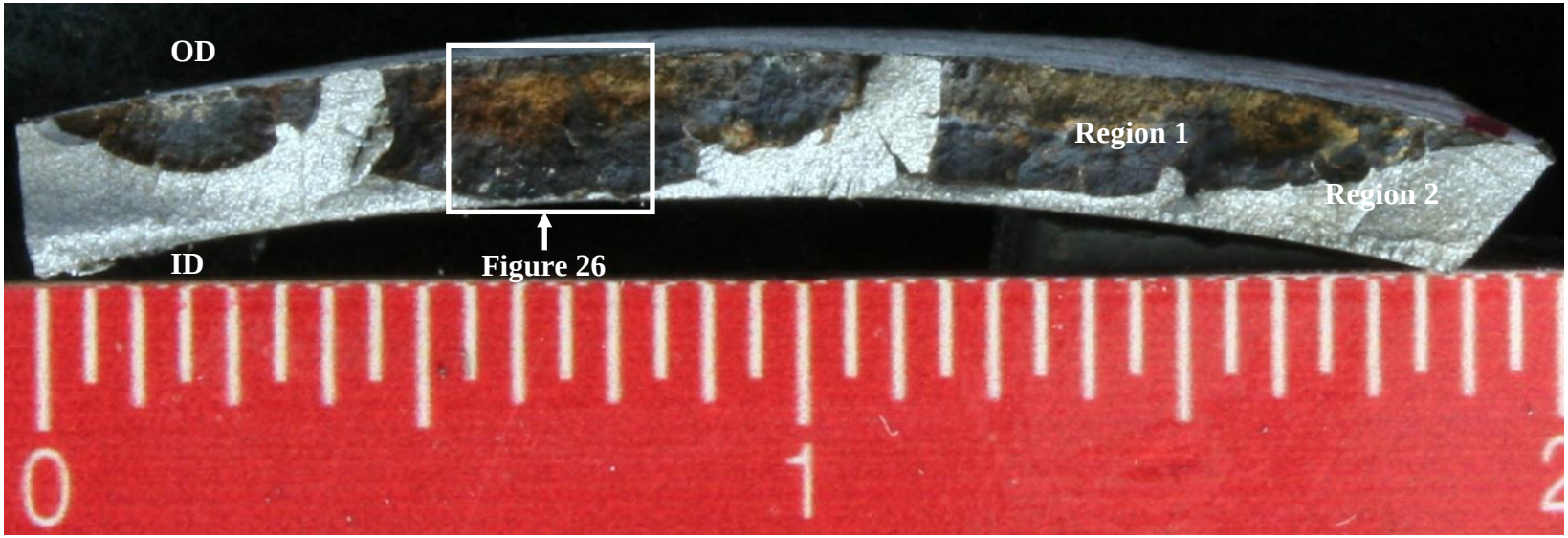

Figure 17. Photograph of the fracture surface removed from Crack Colony 2.

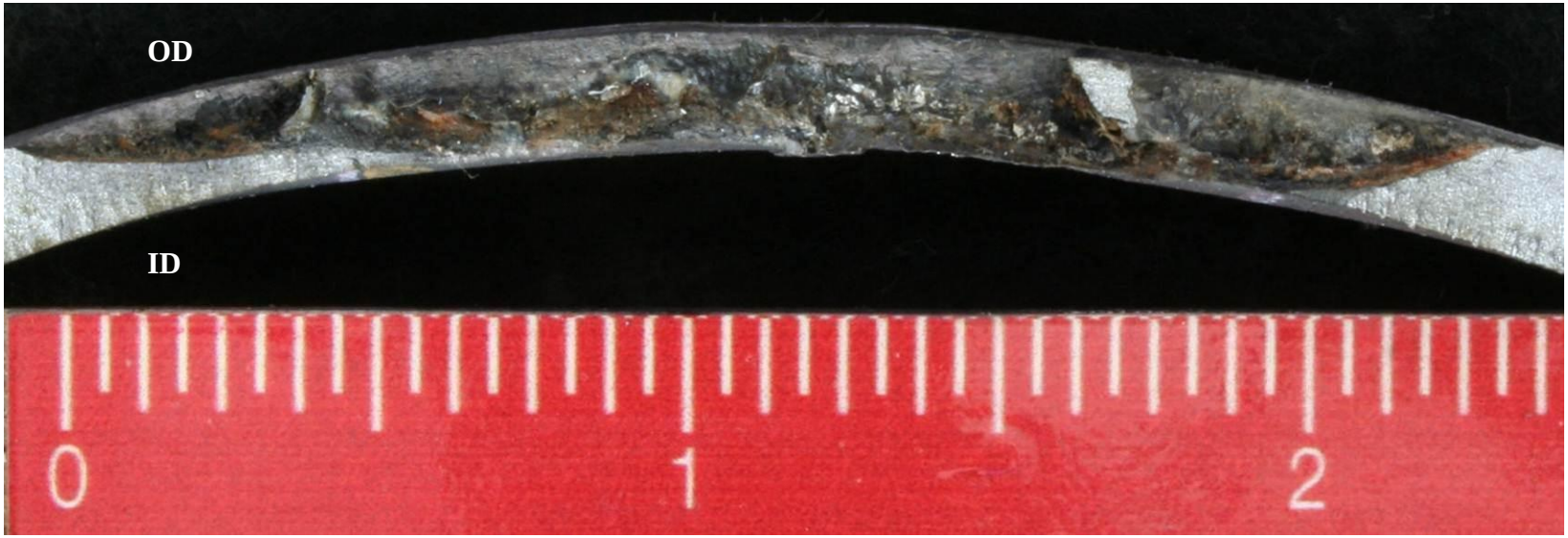

Figure 18. Photograph of the fracture surface removed from Crack Colony 4.

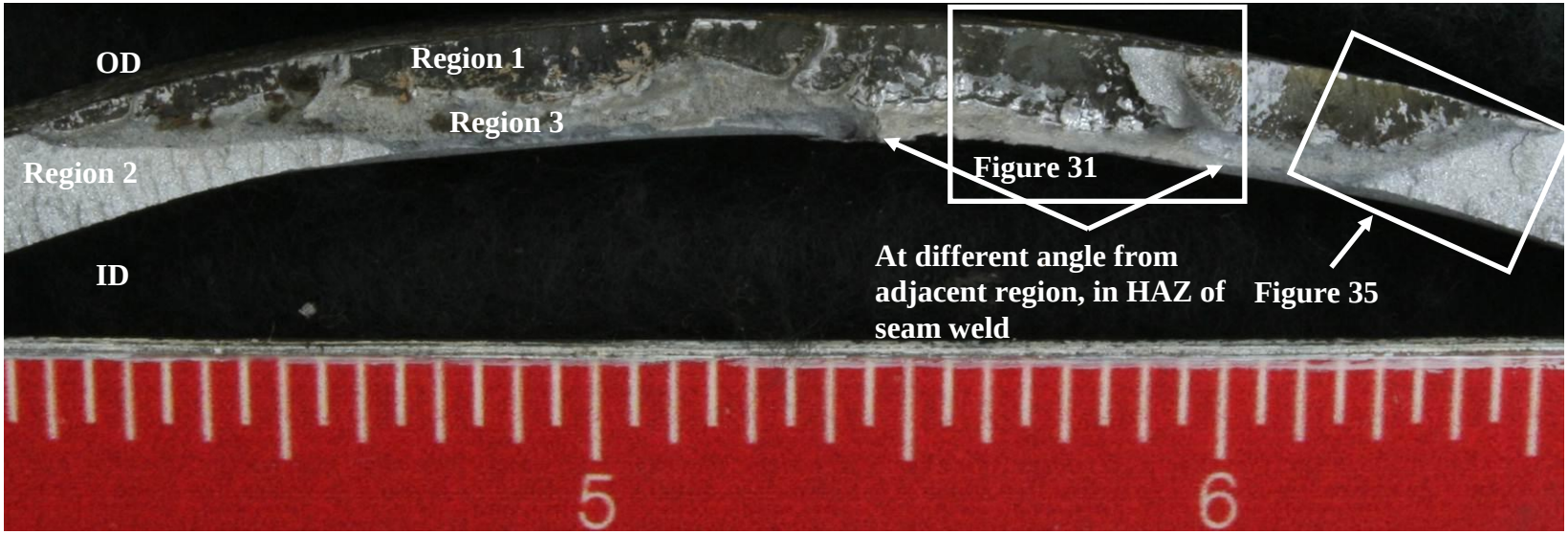

Figure 19. Photograph of the fracture surface removed from Crack Colony 4 after mild cleaning in Endox.

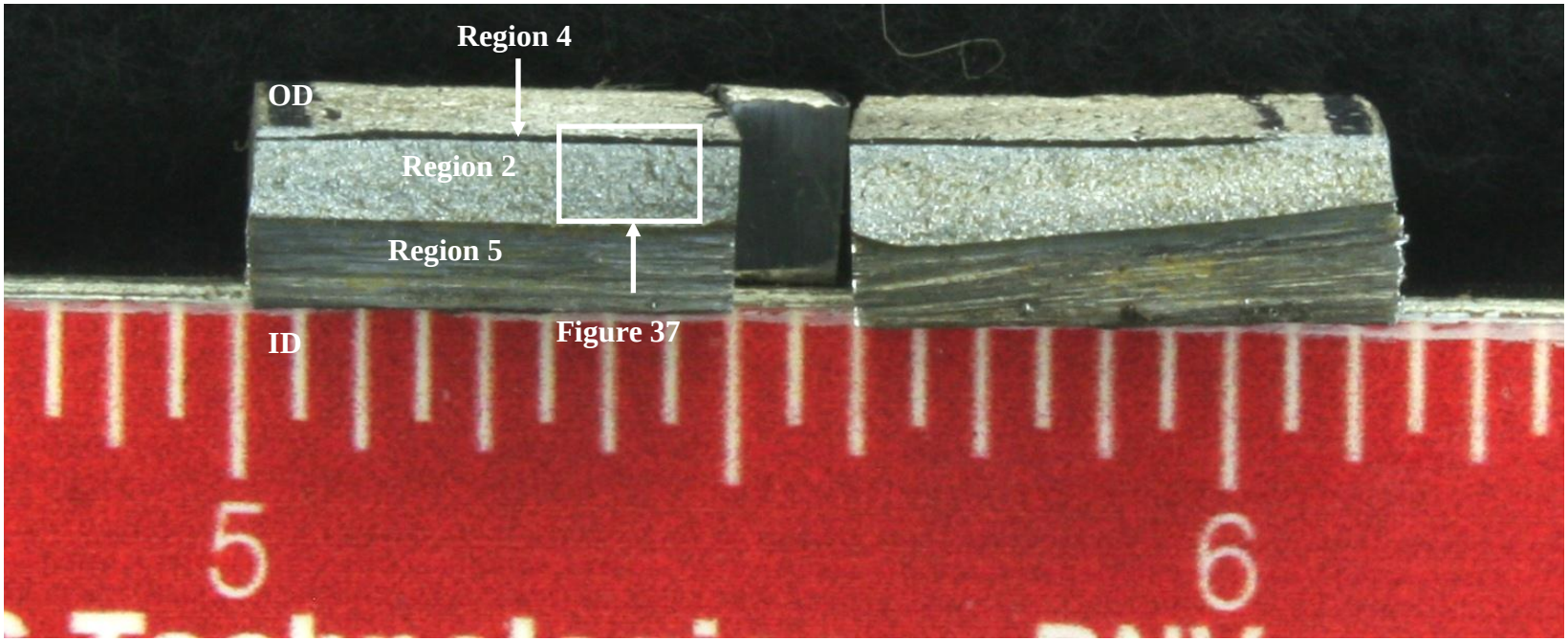

Figure 20. Photograph of the fracture surface removed from the feature near Crack Colony 5.

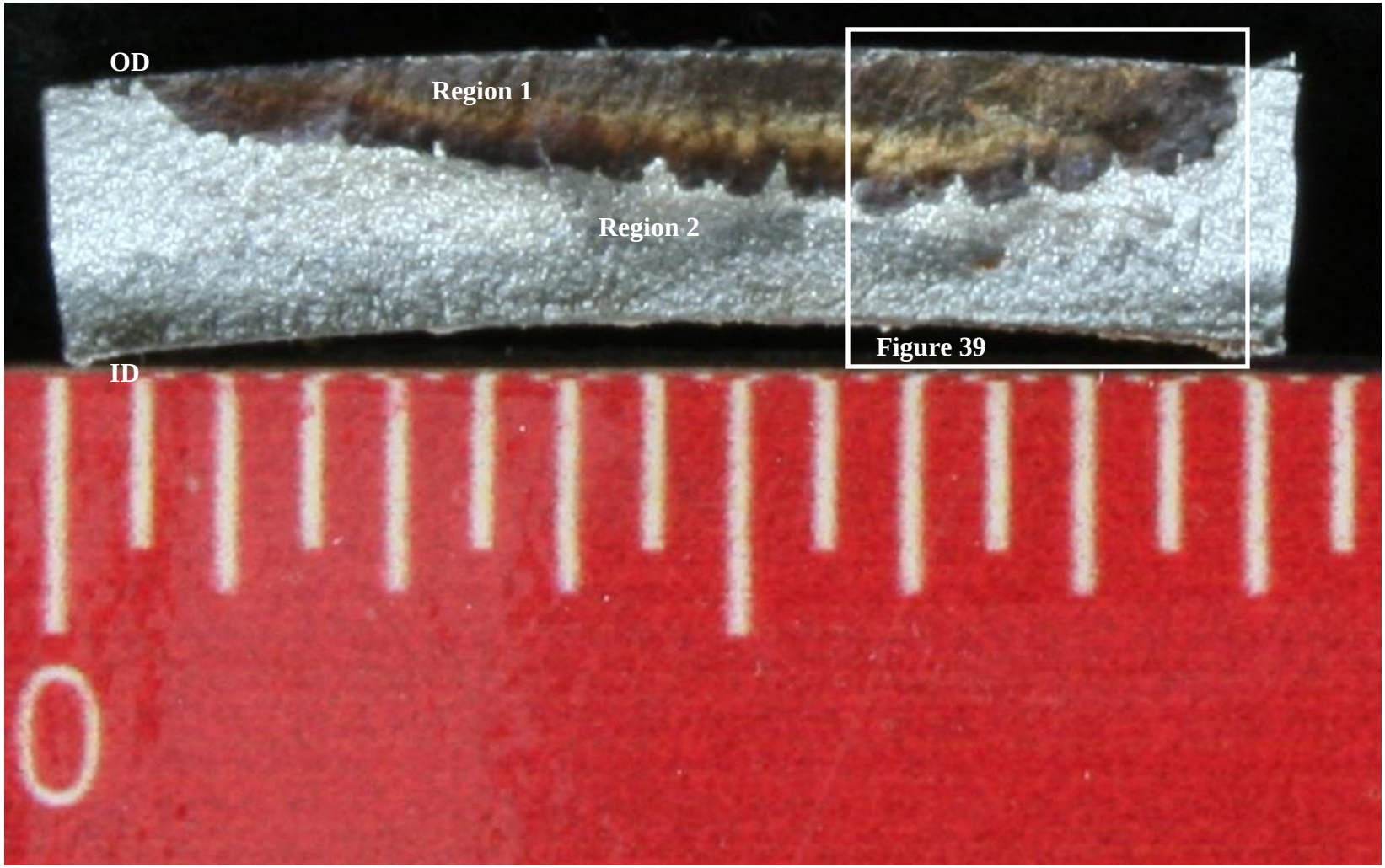

Figure 21. Photograph of the fracture surface removed from Crack Colony 6A.

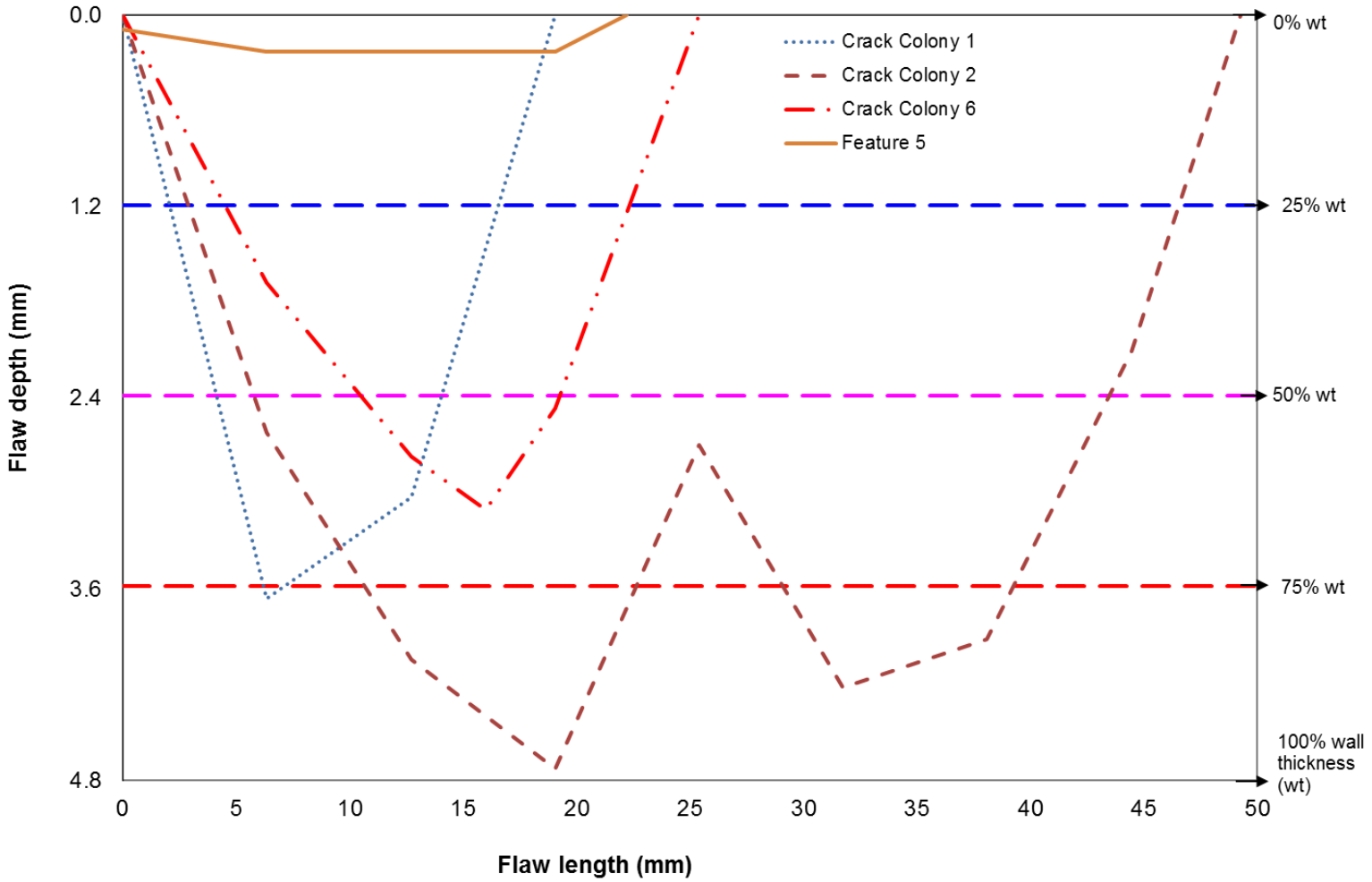

Figure 22. Flaw depth versus flaw length for three of the thumbnail shaped cracks, and a feature, located at/near the crack colonies.

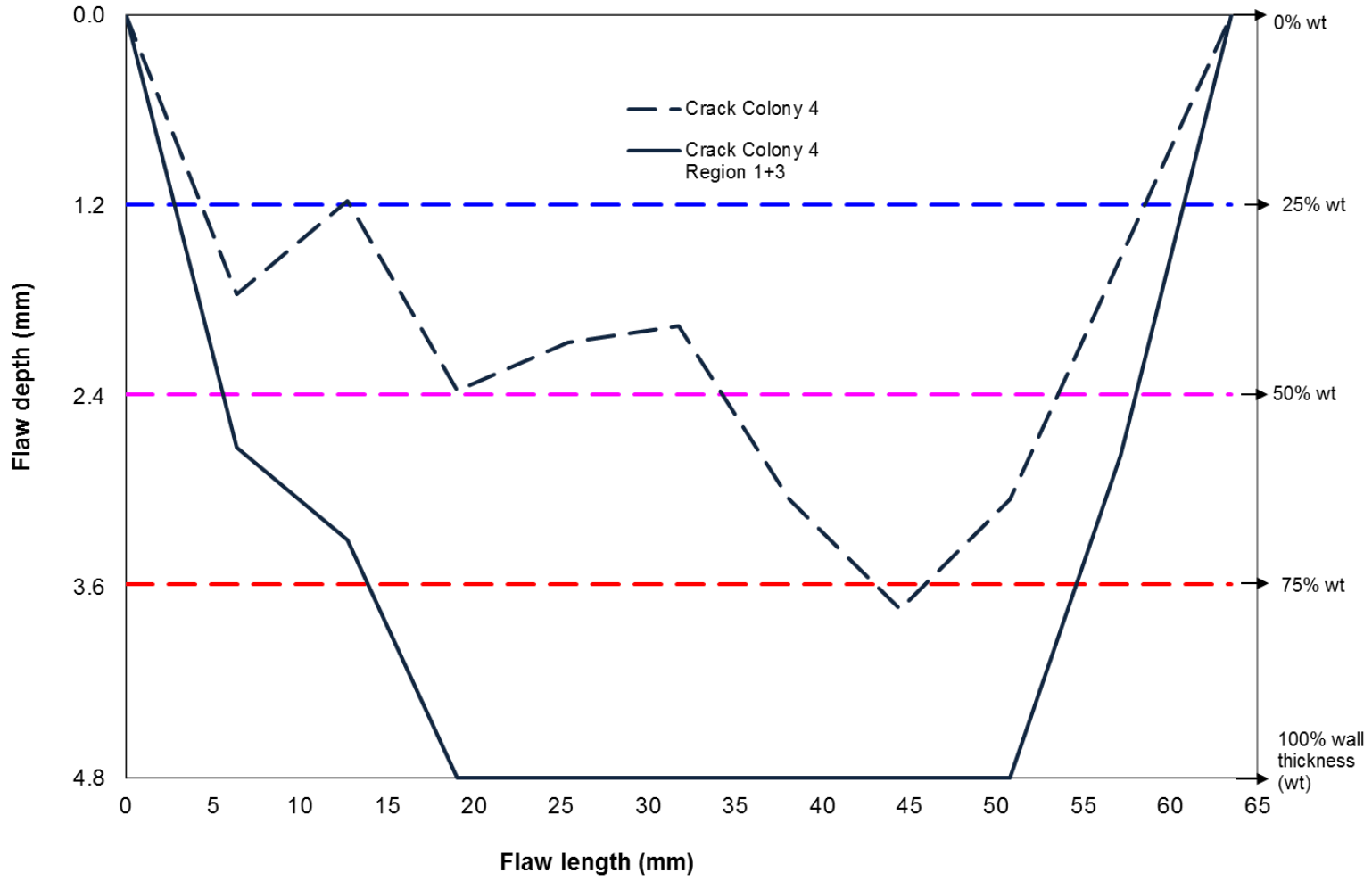

Figure 23. Flaw depth versus flaw length for the thumbnail shaped cracks and overload region at the leak location.

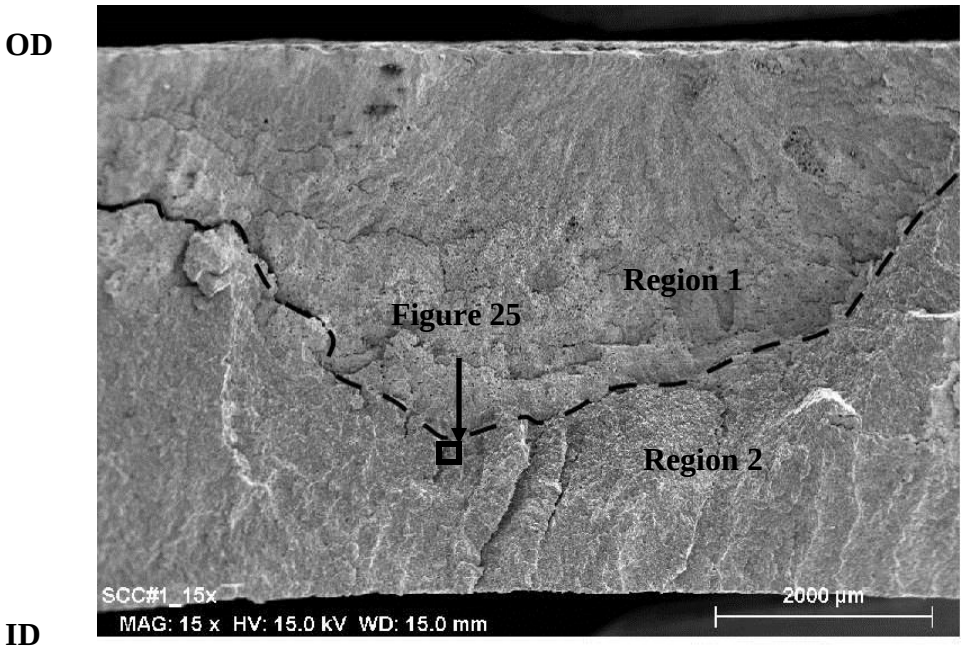

Figure 24. SEM image of fracture surface Sample S1 from Colony 1; mating surface indicated in Figure 16.

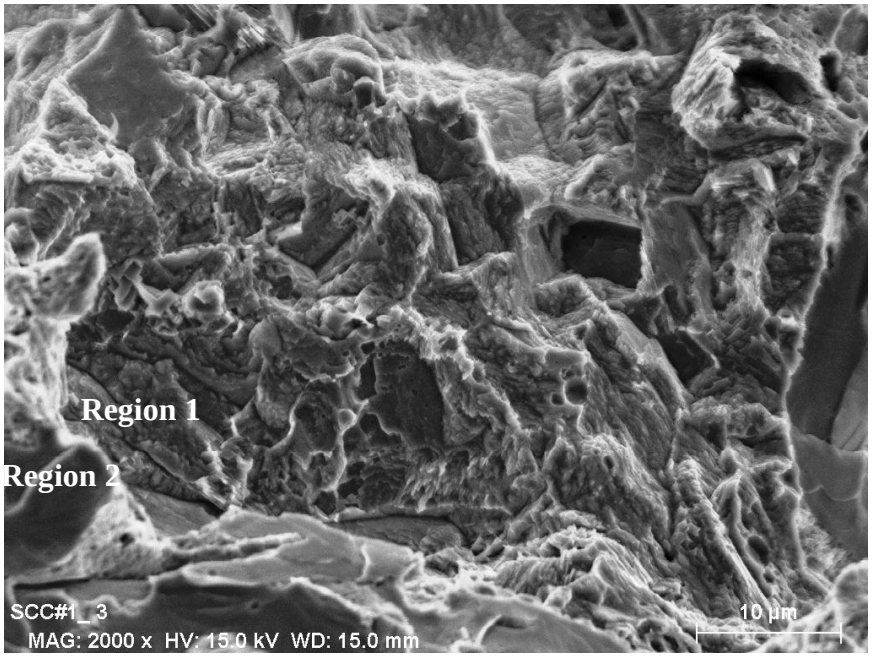

Figure 25. High magnification SEM image of the fracture surface of Sample S1 in the thumbnail crack (Region 1) and brittle overload region (Region 2); area indicated in Figure 24.

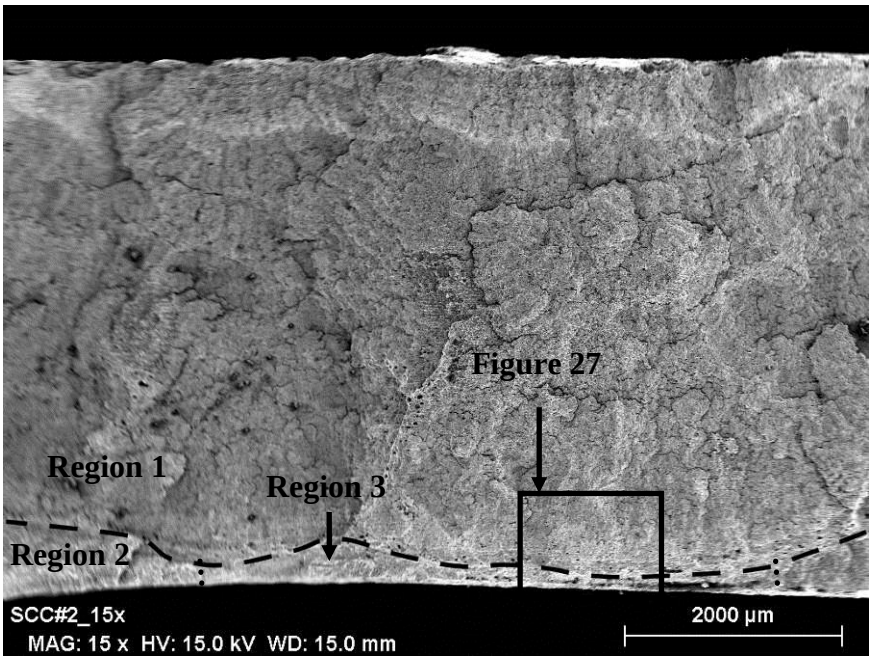

Figure 26. SEM image of fracture surface Sample S2 from Colony 2; mating surface indicated in Figure 16.

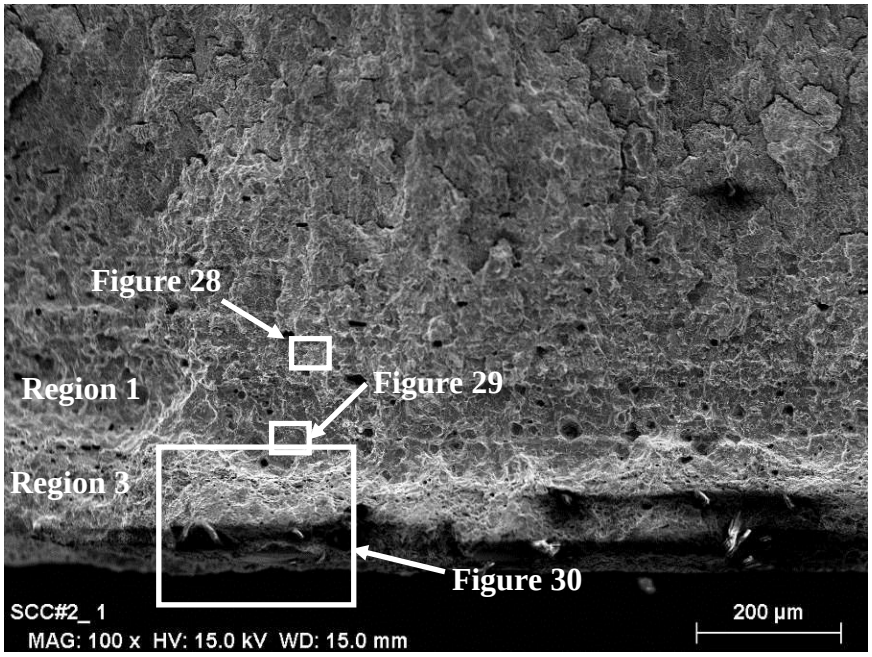

Figure 27. SEM image of the fracture surface of Sample S2 near the ID surface; area indicated in Figure 26.

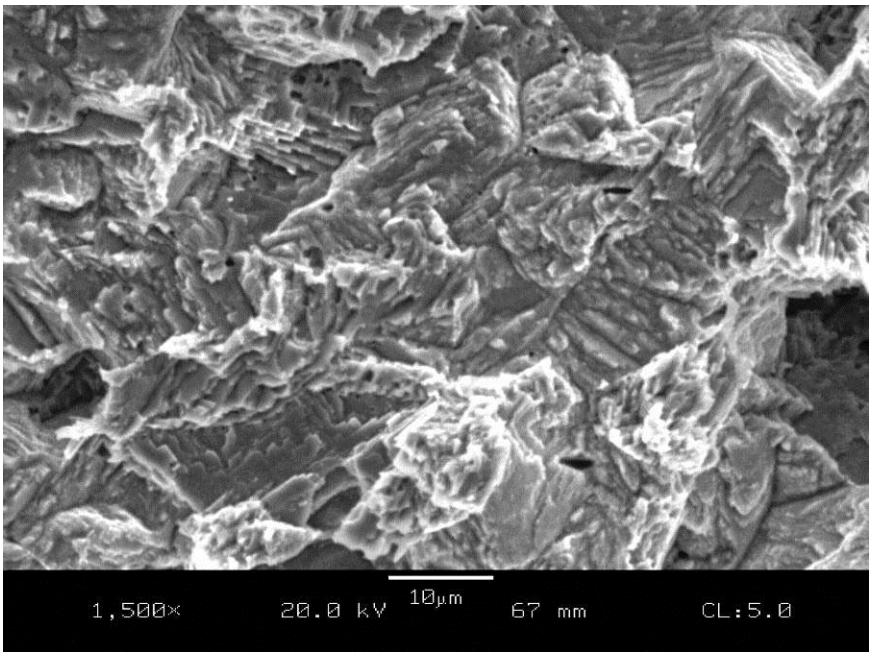

Figure 28. High magnification SEM image of the fracture surface of Sample S2 in the thumbnail crack region (Region 1); area indicated in Figure 27.

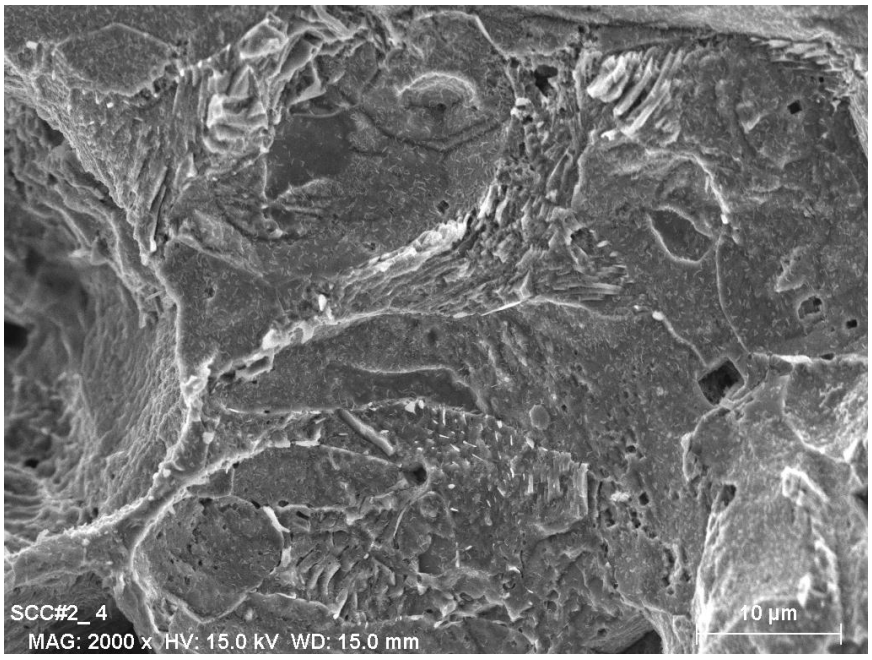

Figure 29. Additional high magnification SEM image of the fracture surface of Sample S2 in the thumbnail crack region (Region 1); area indicated in Figure 27.

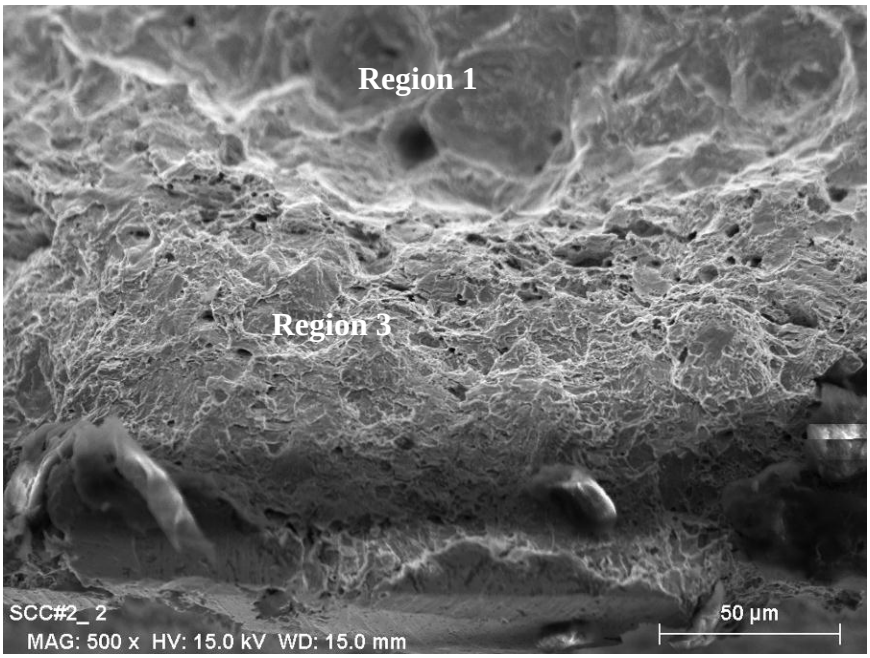

Figure 30. High magnification SEM image of the fracture surface of Sample S2 near the ID surface; area indicated in Figure 27.

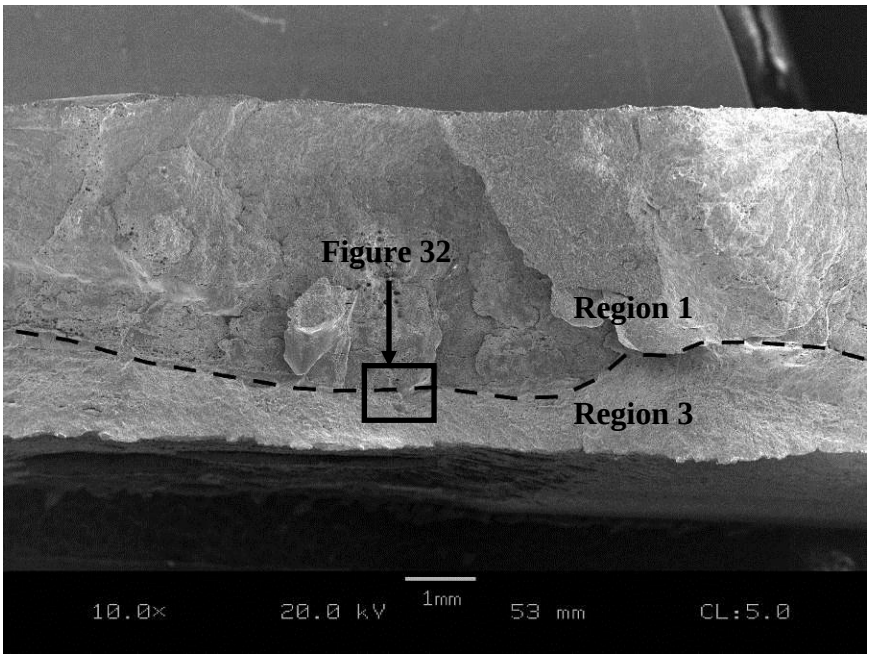

Figure 31. SEM image of fracture surface Sample S4 from Colony 4; area indicated in Figure 19.

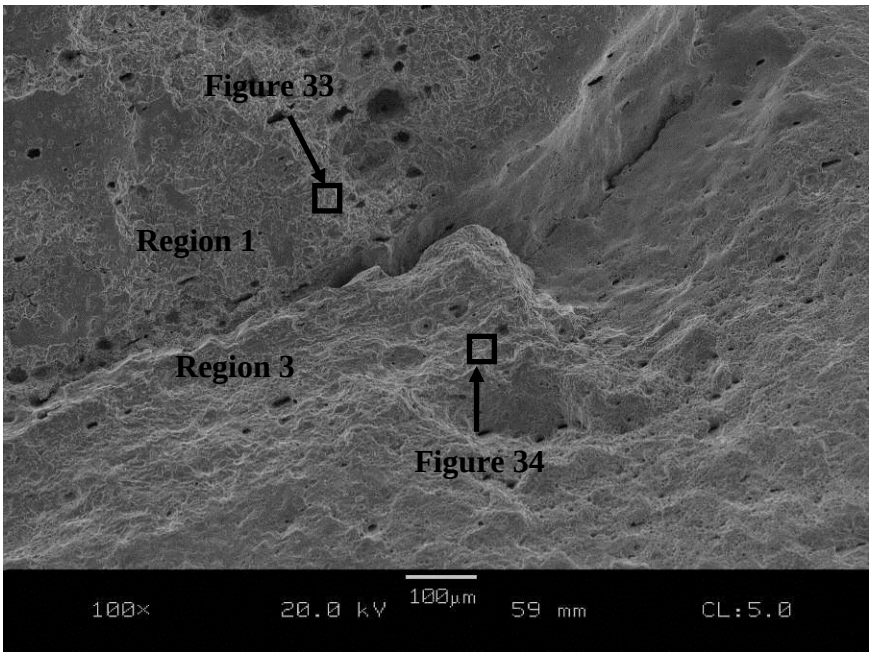

Figure 32. SEM image of the fracture surface of Sample S4 at the thumbnail crack region (Region 1) and ductile overload region (Region 3); area indicated in Figure 31.

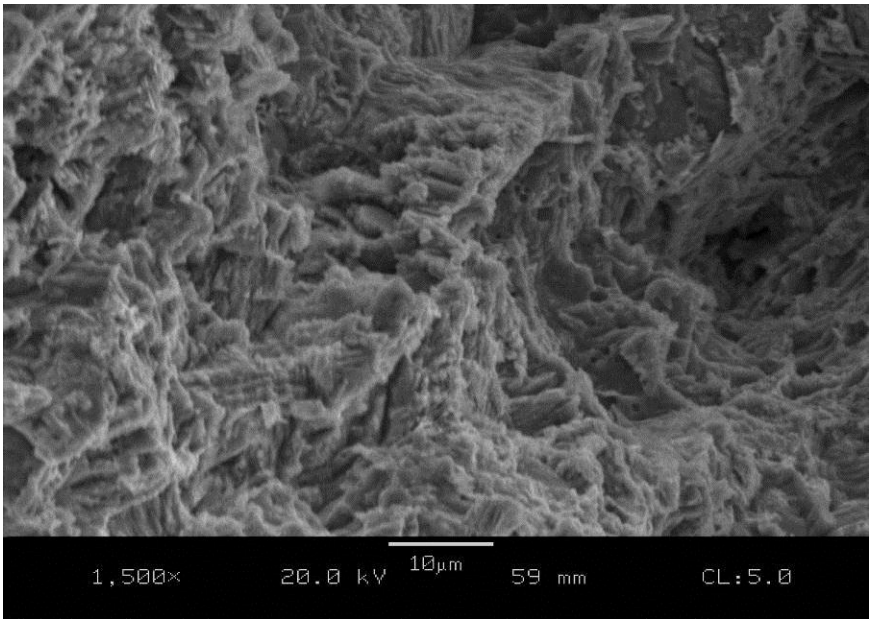

Figure 33. High magnification SEM image of the fracture surface of Sample S4 in the thumbnail crack region (Region 1); area indicated in Figure 32.

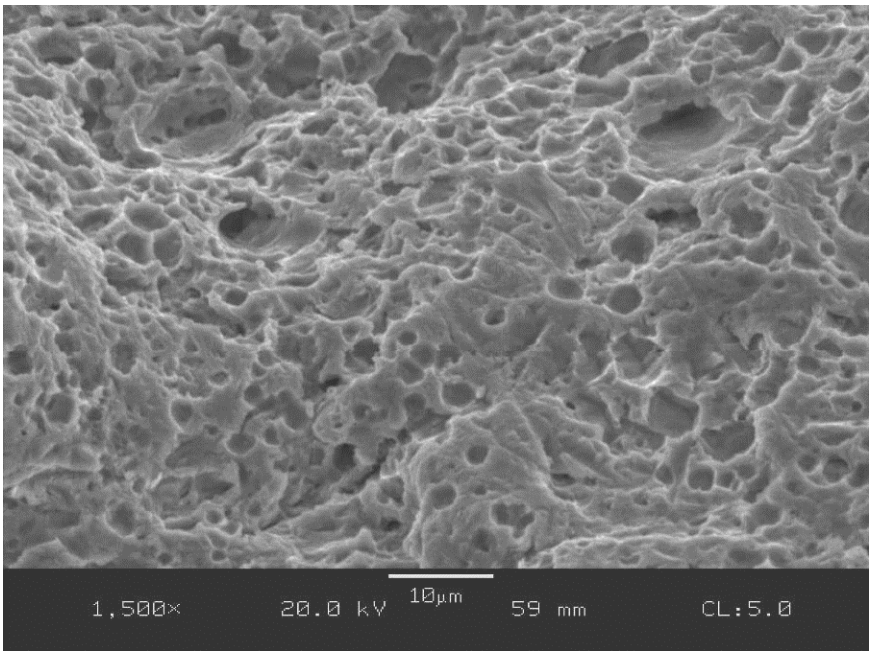

Figure 34. High magnification SEM image of the fracture surface of Sample S4 in the ductile overload region (Region 3); area indicated in Figure 32.

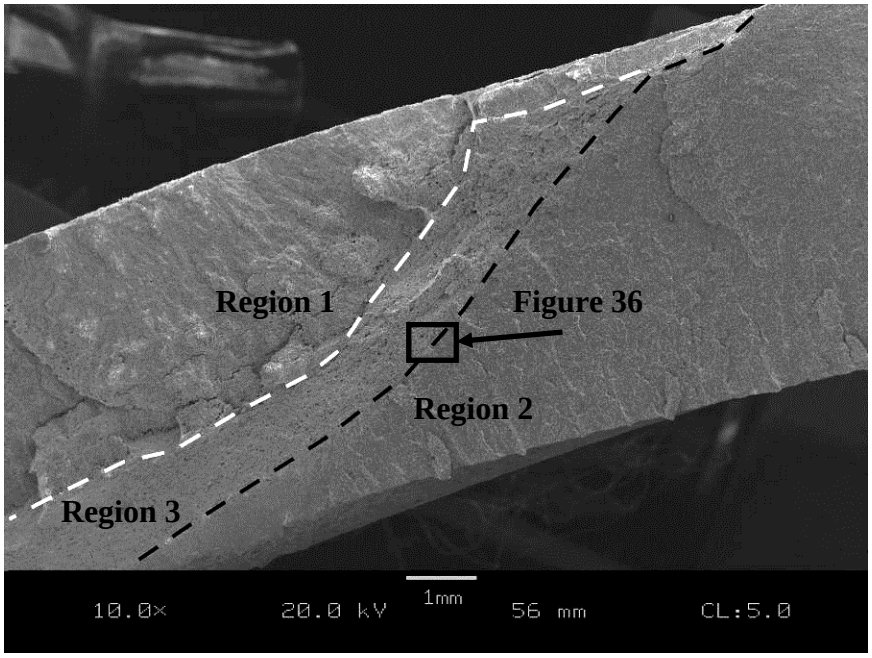

Figure 35. SEM image of the fracture surface of Sample S4 from Colony 4; area indicated in Figure 19.

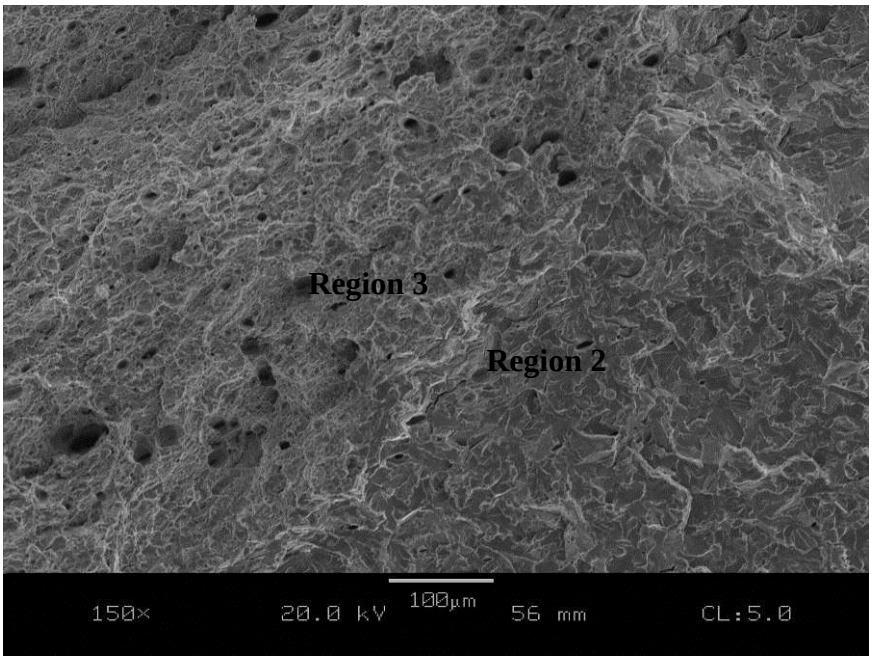

Figure 36. SEM image of the fracture surface of Sample S4 showing the ductile (Region 3) and brittle (Region 2) overload regions; area indicated in Figure 35.

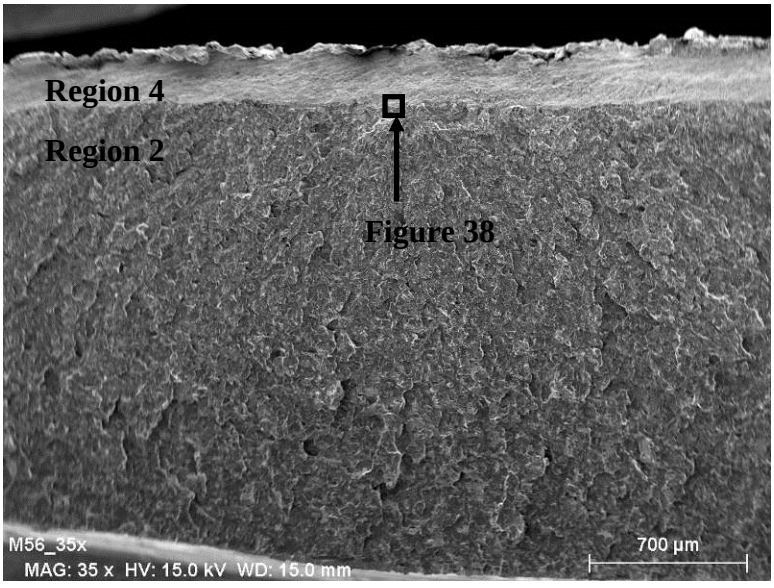

Figure 37. SEM image of fracture surface Sample S5; area indicated in Figure 20.

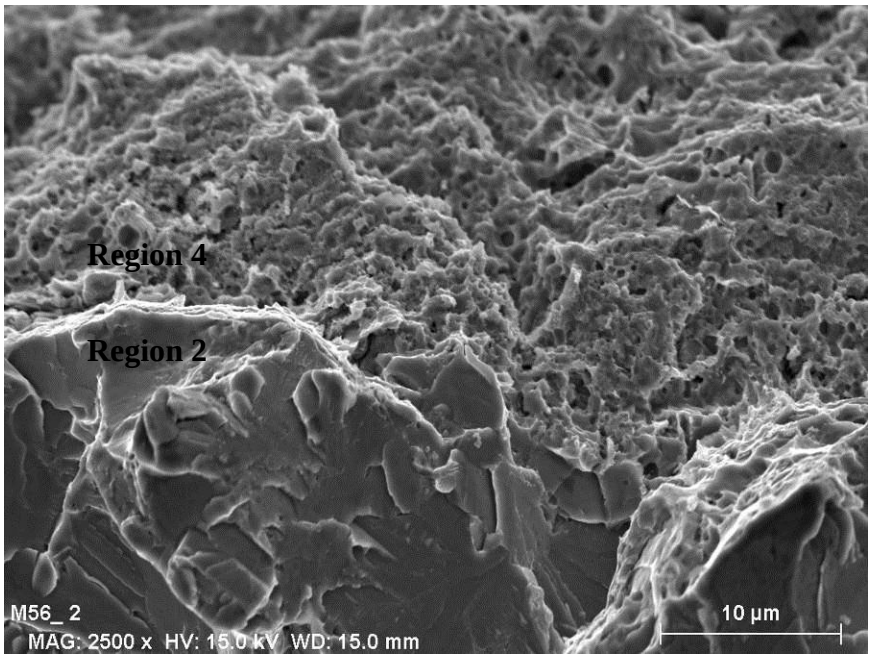

Figure 38. High magnification SEM image of the fracture surface of Sample S5a in the feature region (Region 4) and brittle overload region (Region 2); area indicated in Figure 37.

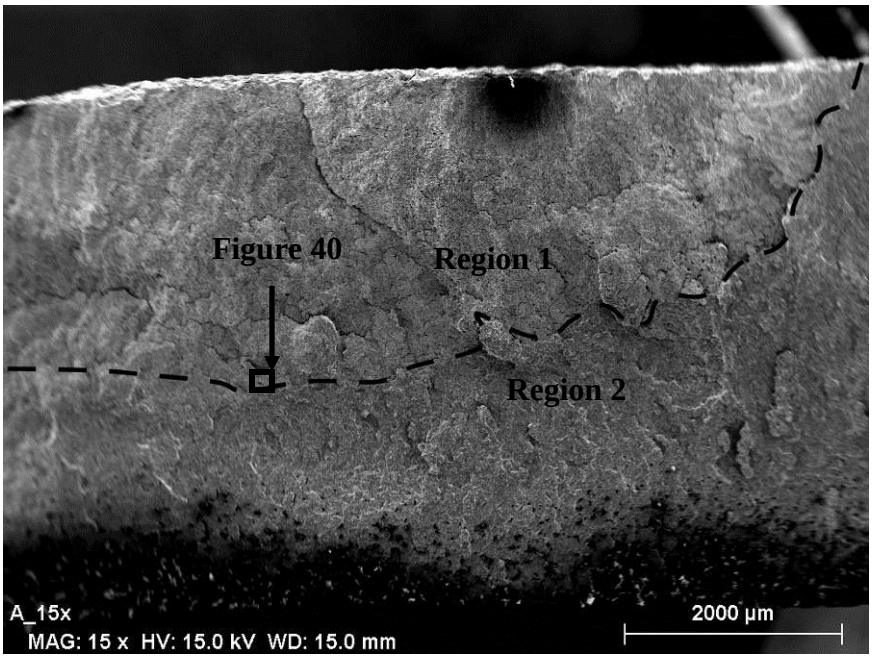

Figure 39. SEM image of fracture surface Sample S6 from Colony 6A; area indicated in Figure 21.

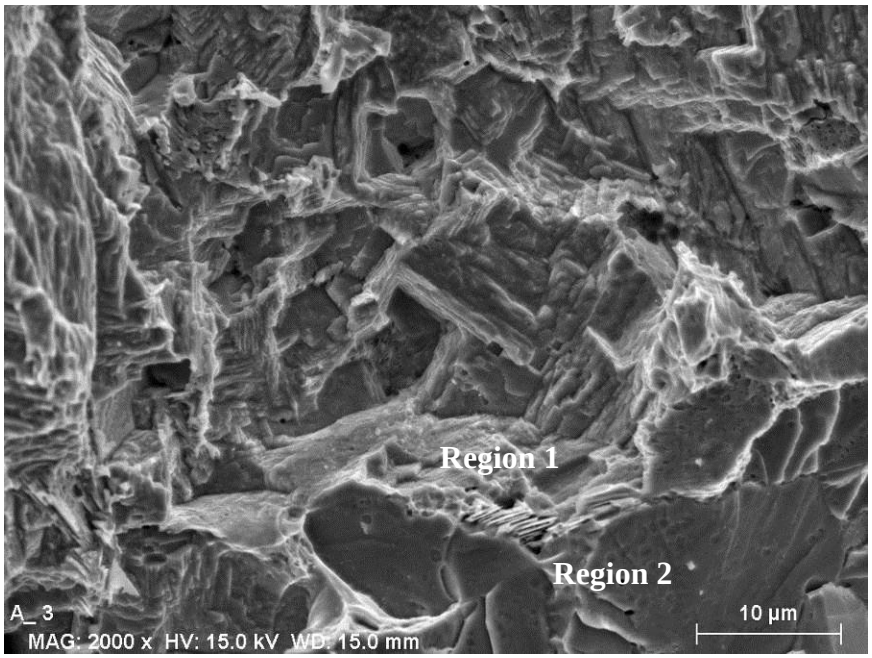

Figure 40. High magnification SEM image of the fracture surface of Sample S6 in the thumbnail crack (Region 1) and brittle overload region (Region 2); area indicated in Figure 39.

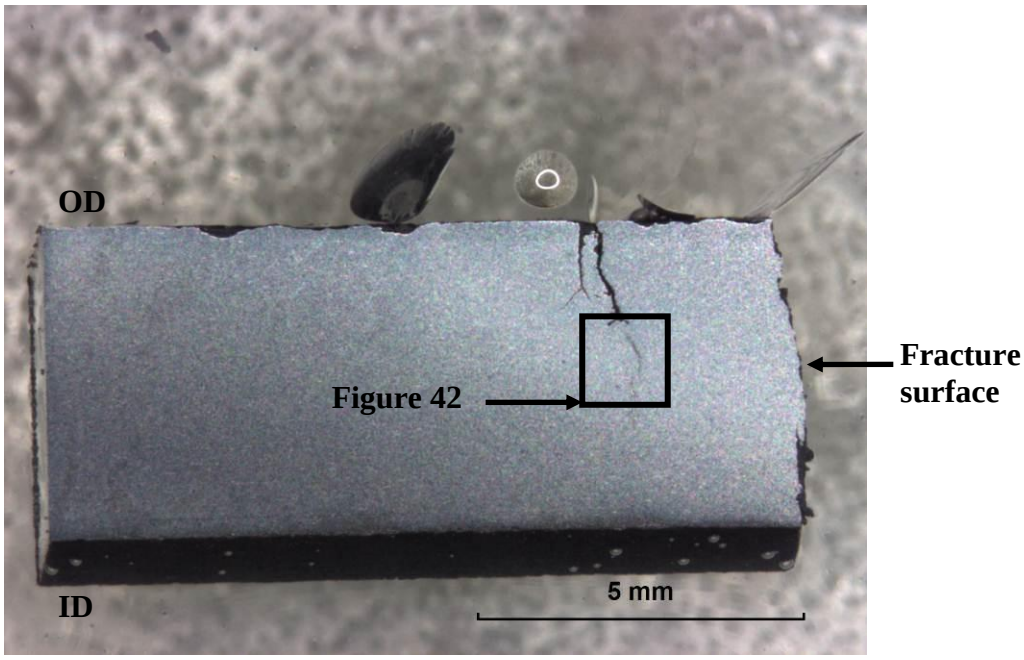

Figure 41. Stereo light photomicrograph of Mount M1 (4% Nital Etchant). Mount was removed from Crack Colony 1.

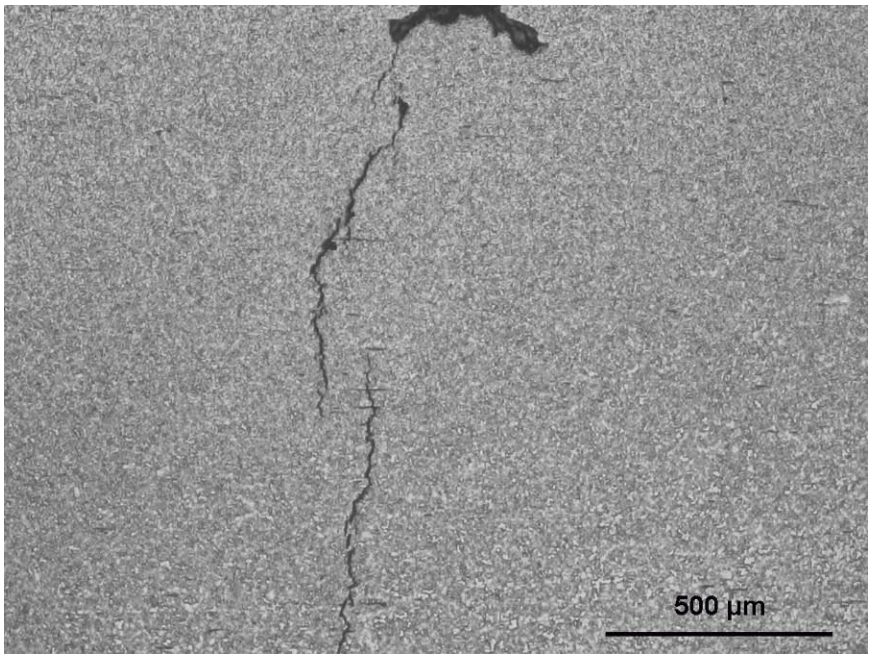

Figure 42. Close-up photomicrograph of Mount M1 (4% Nital Etchant); mirror image of area indicated in Figure 41.

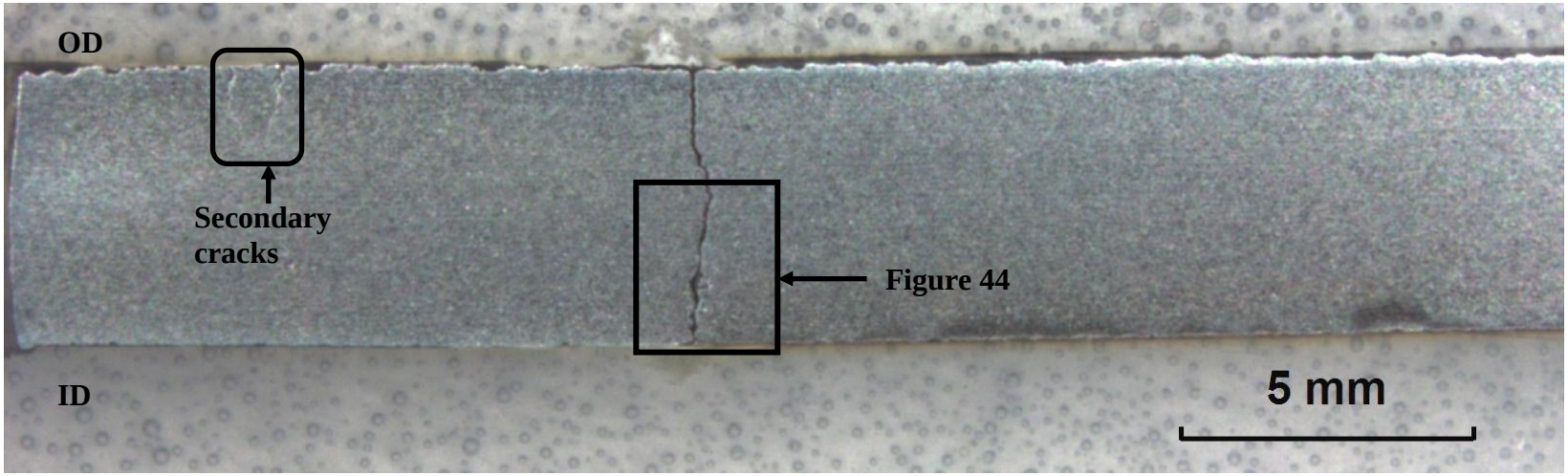

Figure 43. Stereo light photomicrograph of Mount M2 (4% Nital Etchant). Mount was removed from Crack Colony 2 (previously broken open).

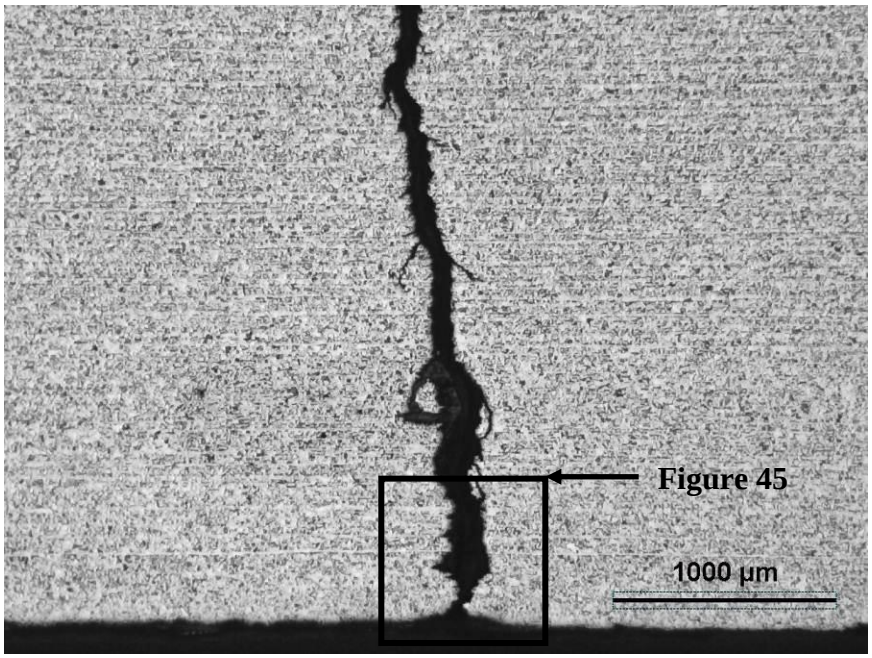

Figure 44. Light photomicrograph of Mount M2 near the ID surface (4% Nital Etchant); mirror image of area indicated in Figure 43.

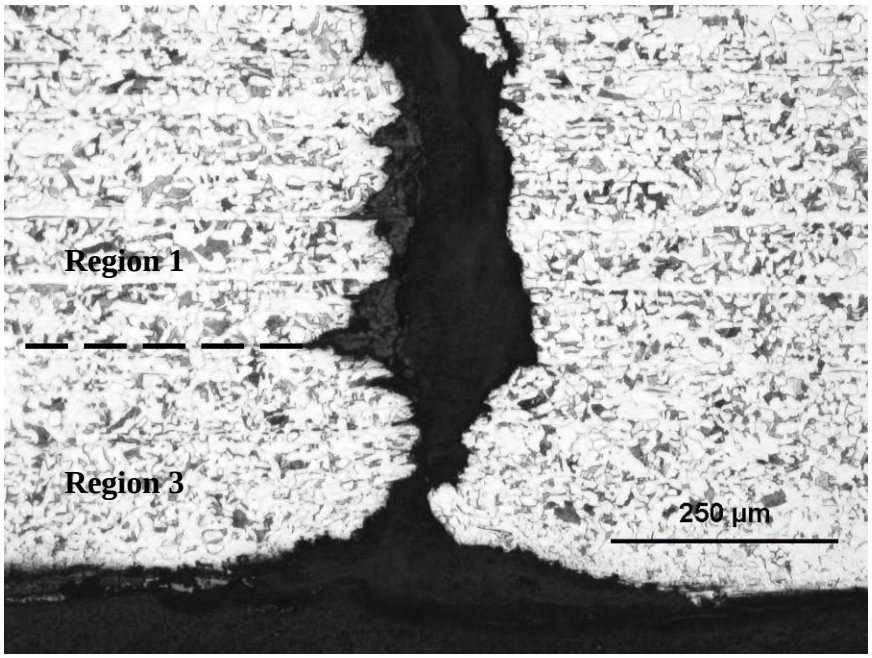

Figure 45. Close-up photomicrograph of Mount M2 near the ID surface (4% Nital Etchant); area indicated in Figure 44.

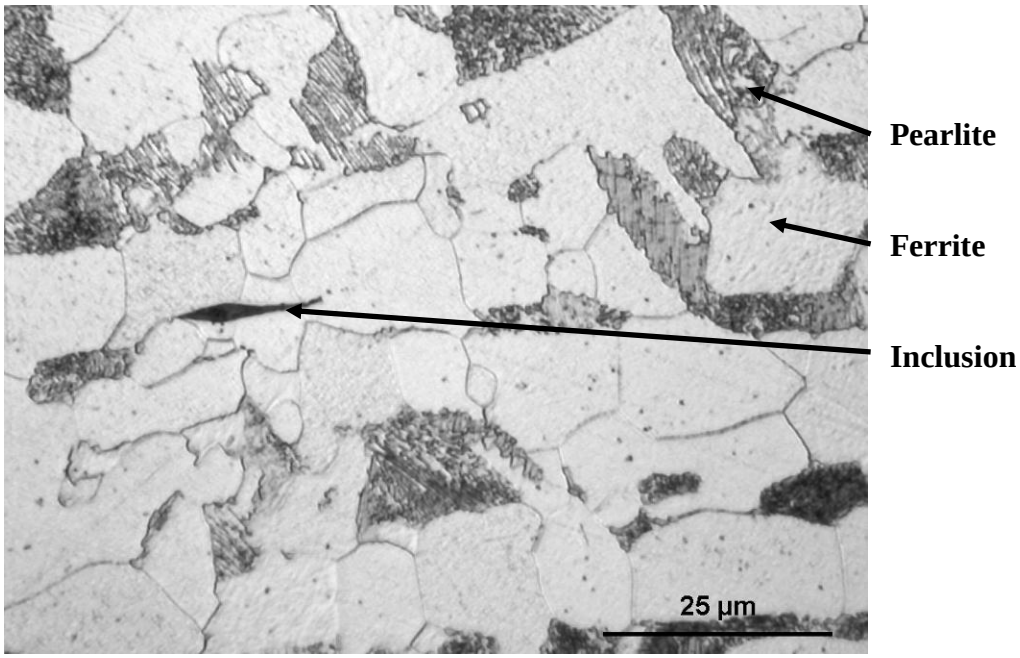

Figure 46. Light photomicrograph of the typical base metal microstructure (Mount M2, 4% Nital Etchant).

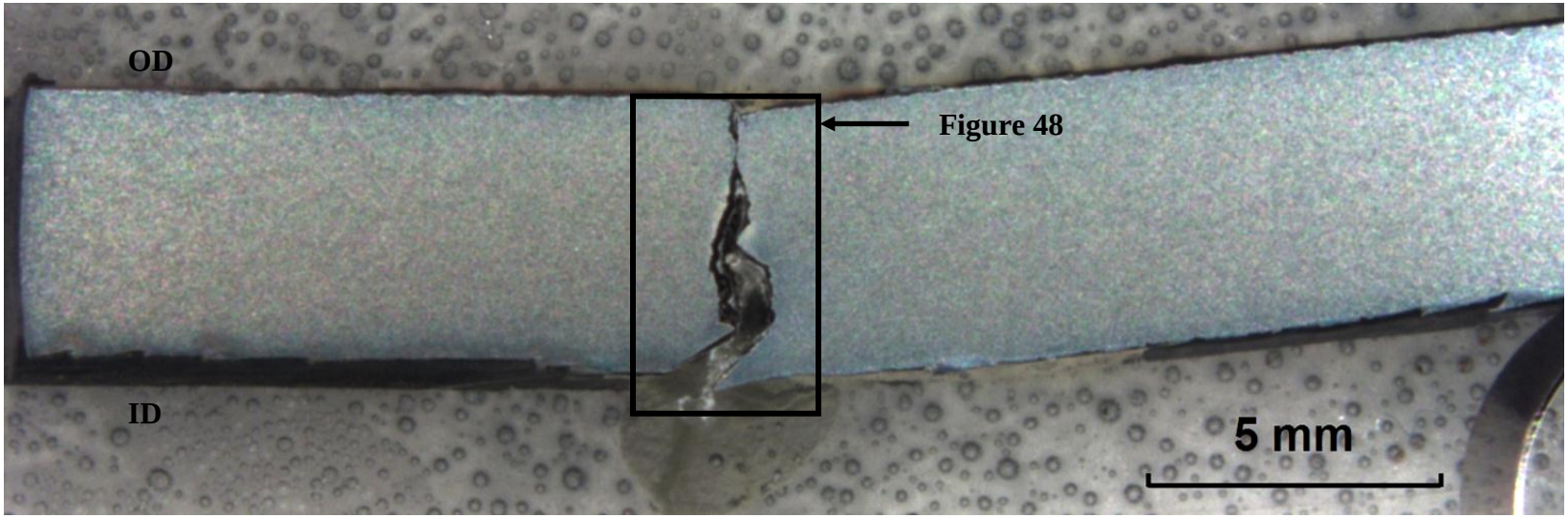

Figure 47. Stereo light photomicrograph of Mount M4 (4% Nital Etchant). Mount was removed from Crack Colony 4.

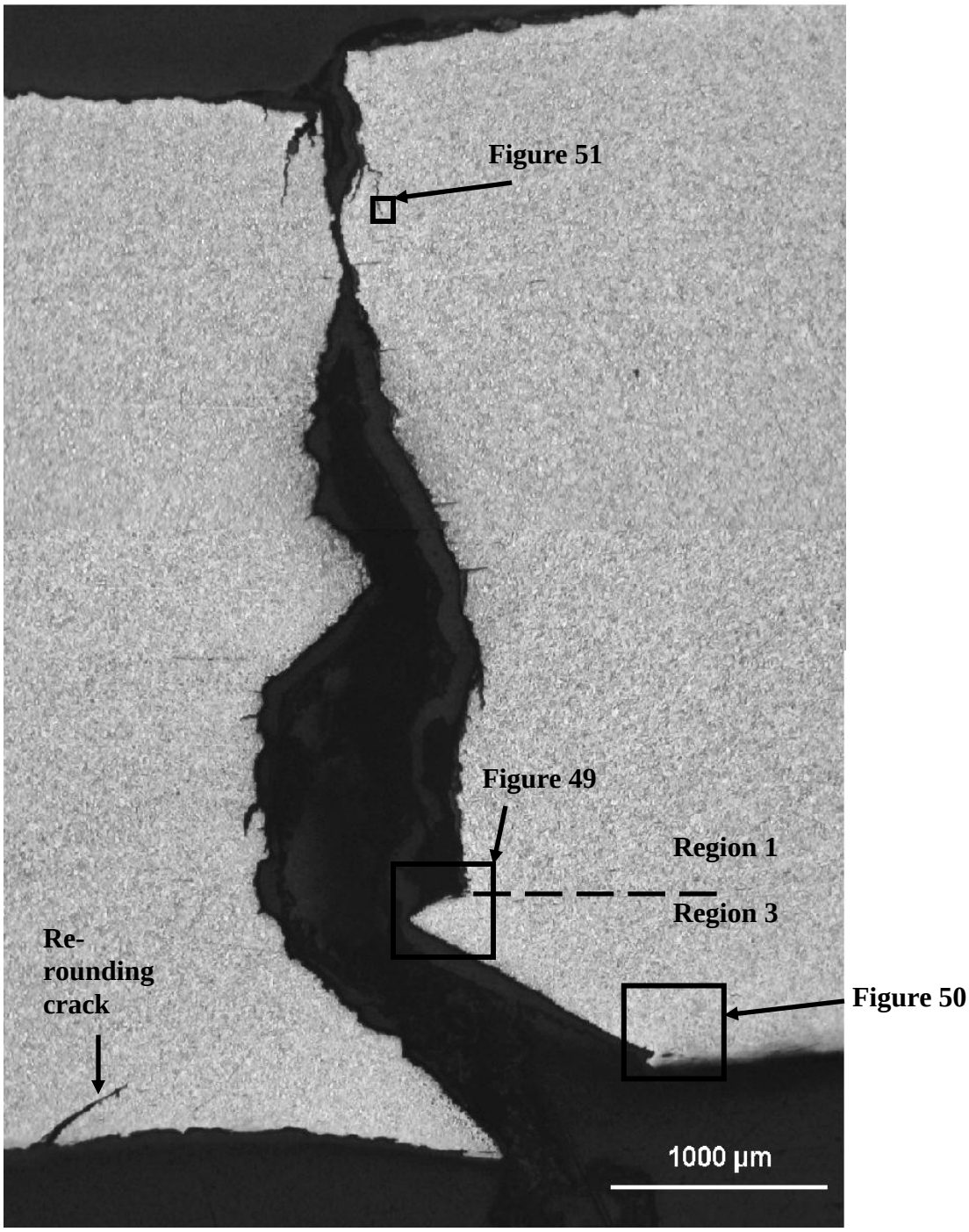

Figure 48. Light photomicrograph of Mount M4 (4% Nital Etchant); mirror image of area indicated in Figure 47.

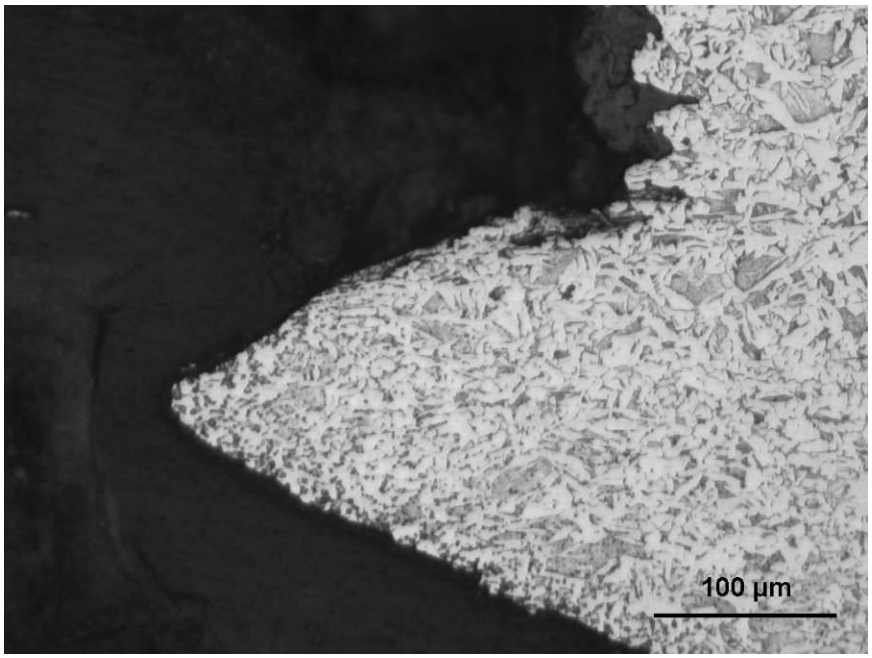

Figure 49. Close-up photomicrograph of Mount M4 at the interface of Region 1 and 3 (4% Nital Etchant); area indicated in Figure 48.

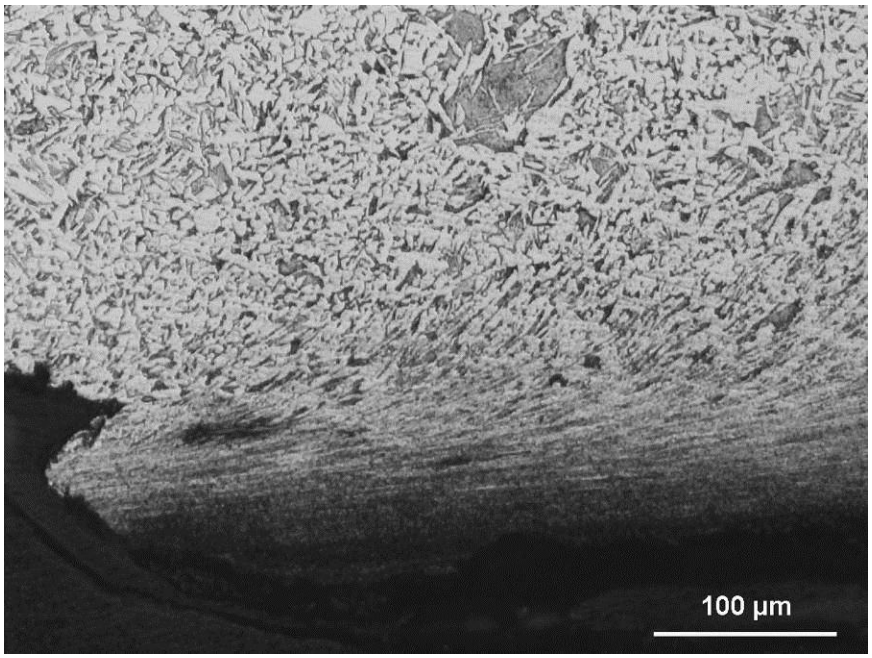

Figure 50. Close-up photomicrograph of Mount M4 showing the ID surface and Region 3 (4% Nital Etchant); area indicated in Figure 48.

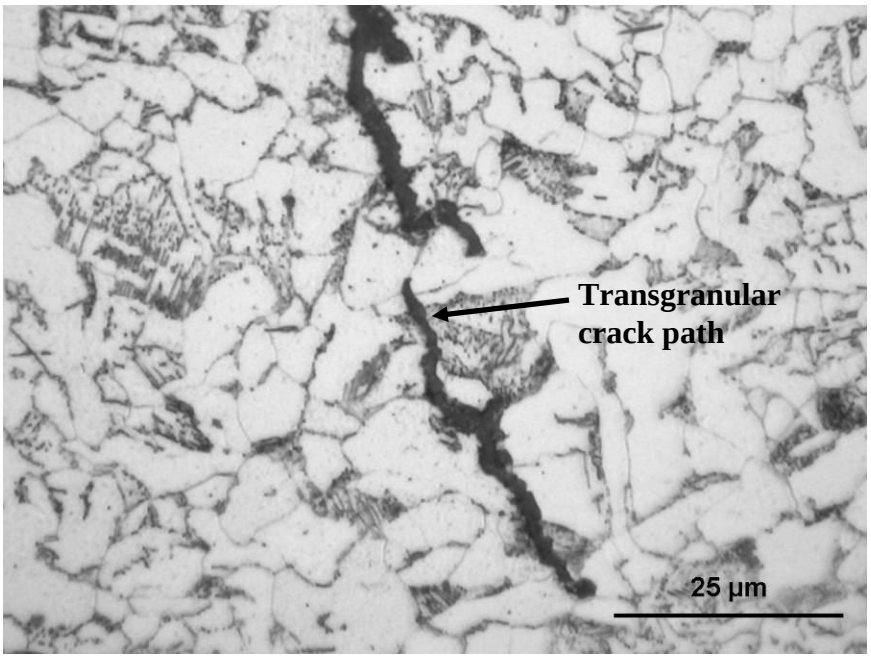

Figure 51. Close-up photomicrograph of Mount M4 showing a crack tip (4% Nital Etchant); area indicated in Figure 48.

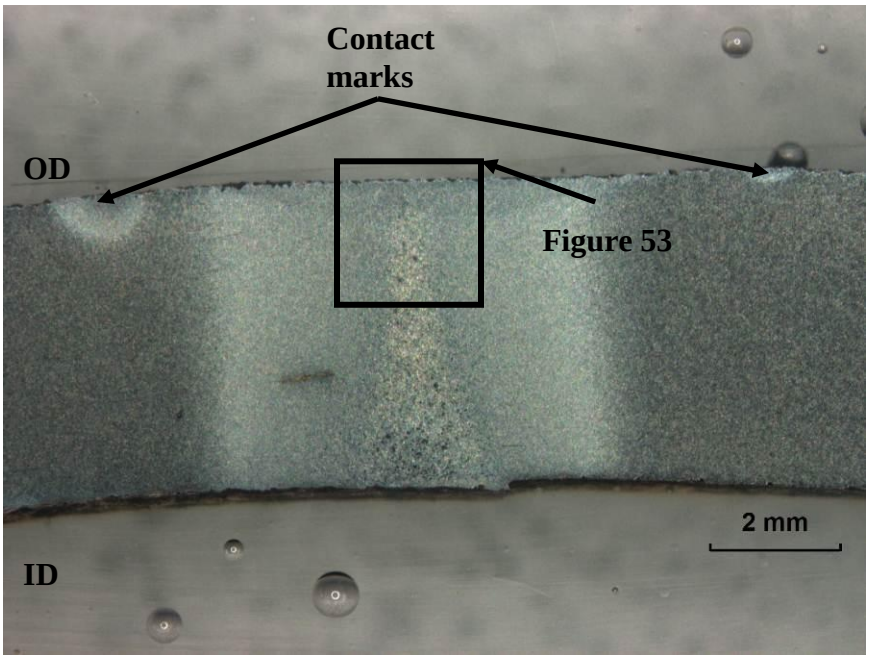

Figure 52. Stereo light photomicrograph of Mount M5a (4% Nital Etchant). Mount was removed near Crack Colony 5a.

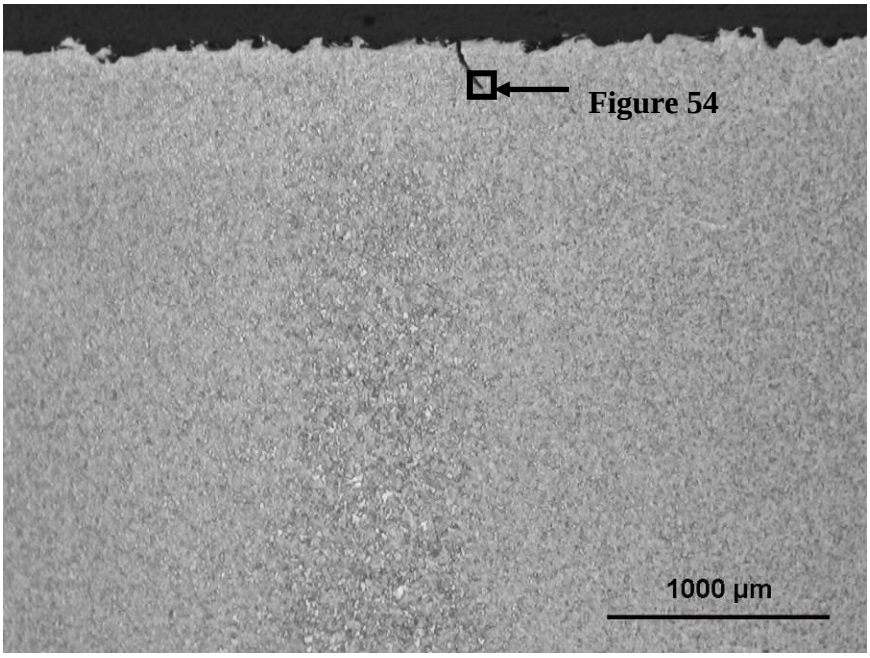

Figure 53. Light photomicrograph of Mount M5a showing a hook crack (4% Nital Etchant); mirror image of area indicated in Figure 52.

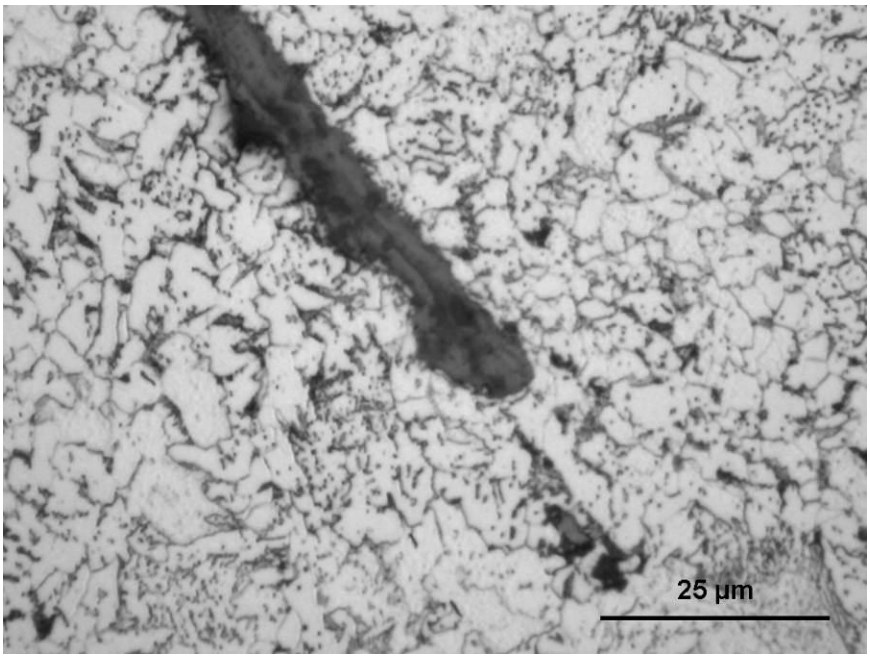

Figure 54. Close-up photomicrograph of Mount M5a showing a crack tip (4% Nital Etchant); area indicated in Figure 53.

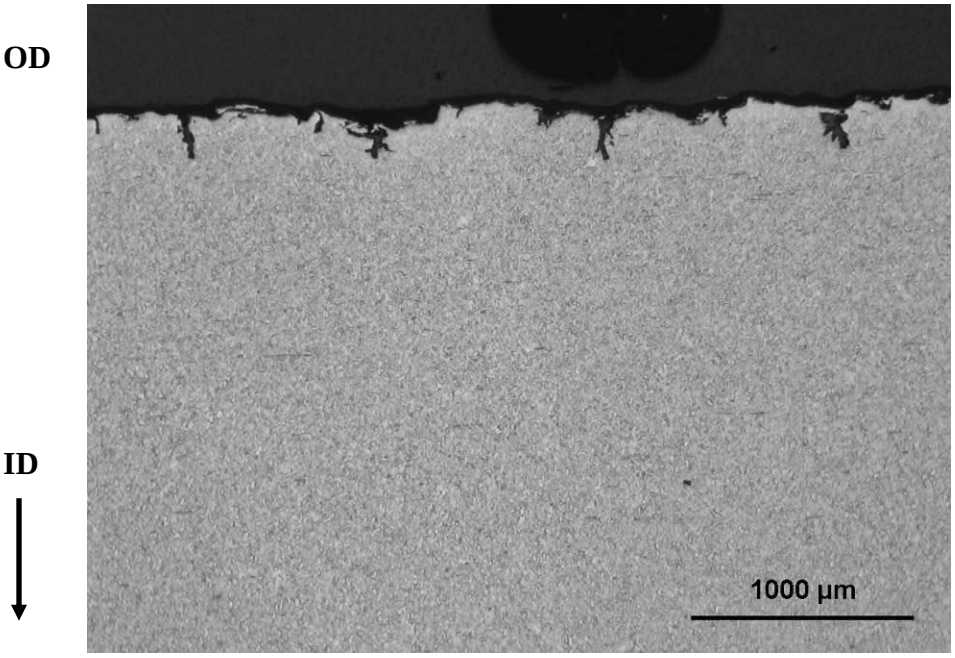

Figure 55. Light photomicrograph of Mount M5b showing secondary cracks (4% Nital Etchant). Mount was removed from Crack Colony 5b.

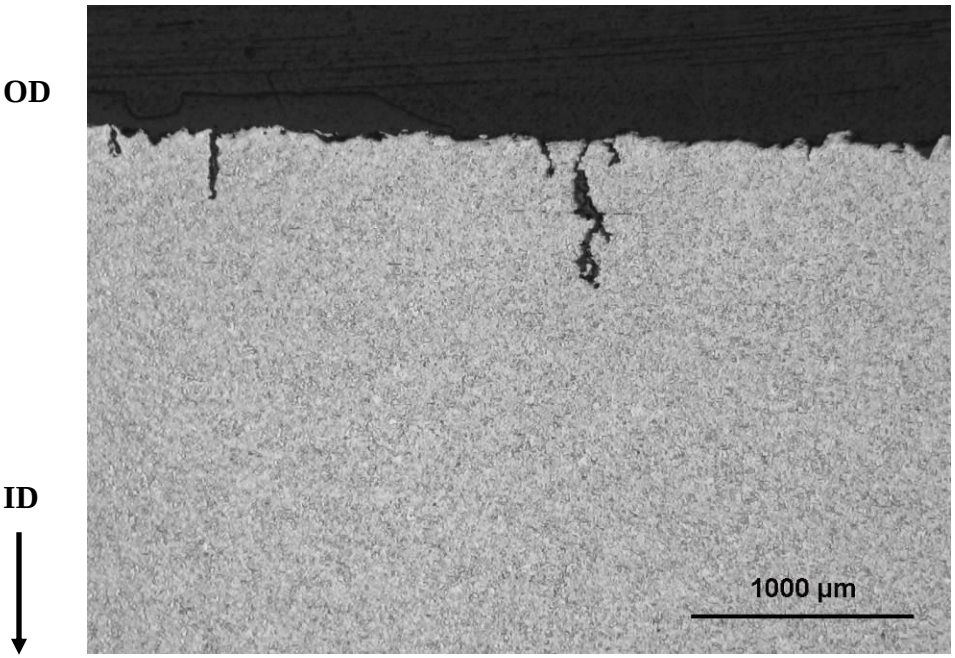

Figure 56. Light photomicrograph of Mount M6 showing secondary cracks (4% Nital Etchant). Mount was removed from Crack Colony 6.

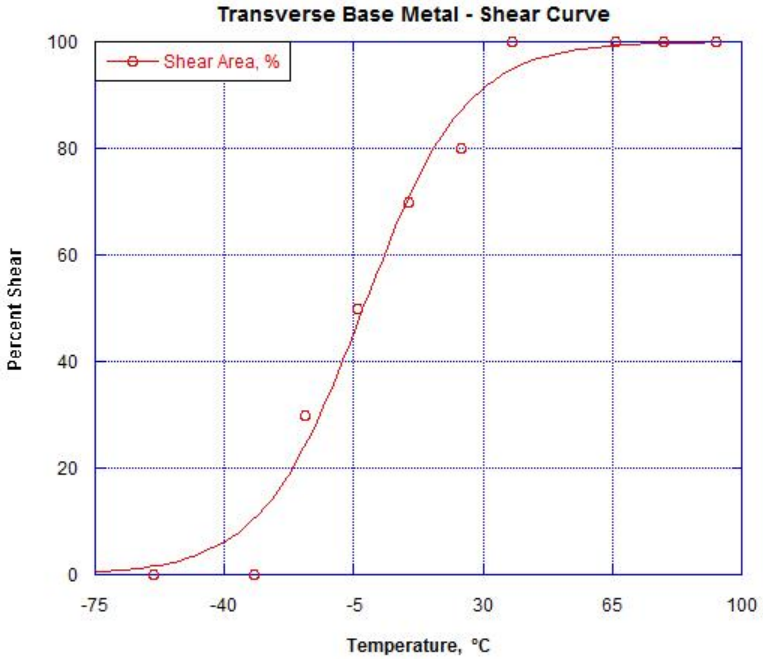

Figure 57. Percent shear from Charpy V-notch tests as a function of temperature for transverse base metal samples removed from the pipe section.

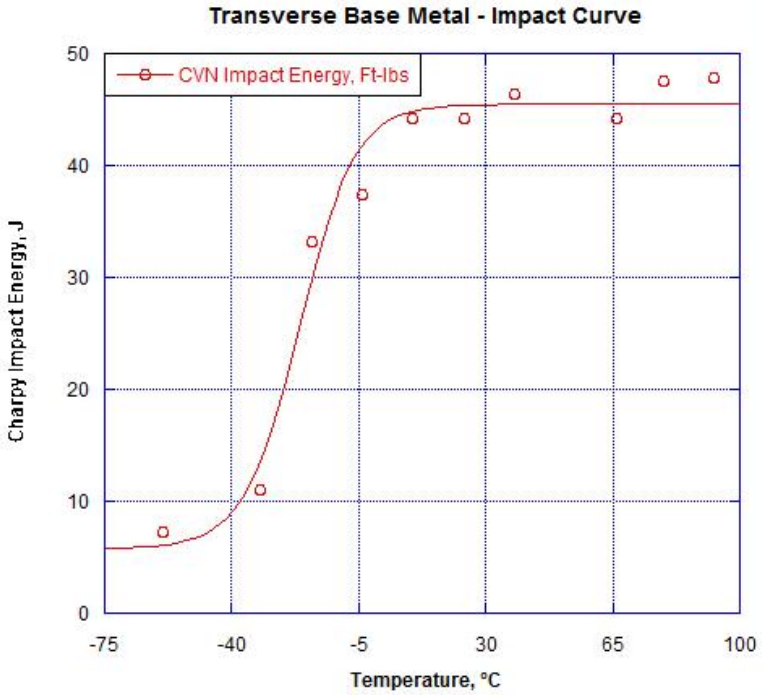

Figure 58. Charpy V-notch impact energy as a function of temperature for transverse base metal samples removed from the pipe section.

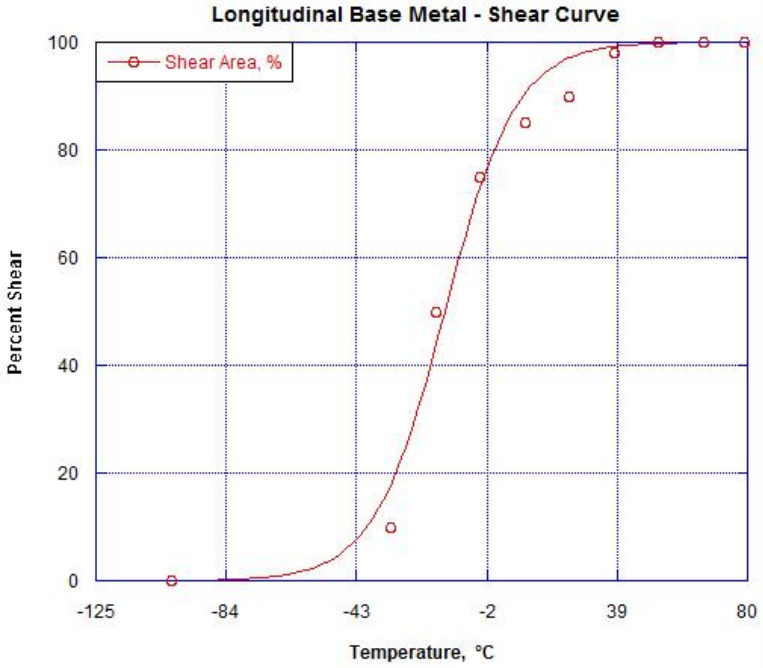

Figure 59. Percent shear from Charpy V-notch tests as a function of temperature for axial base metal samples removed from the pipe section.

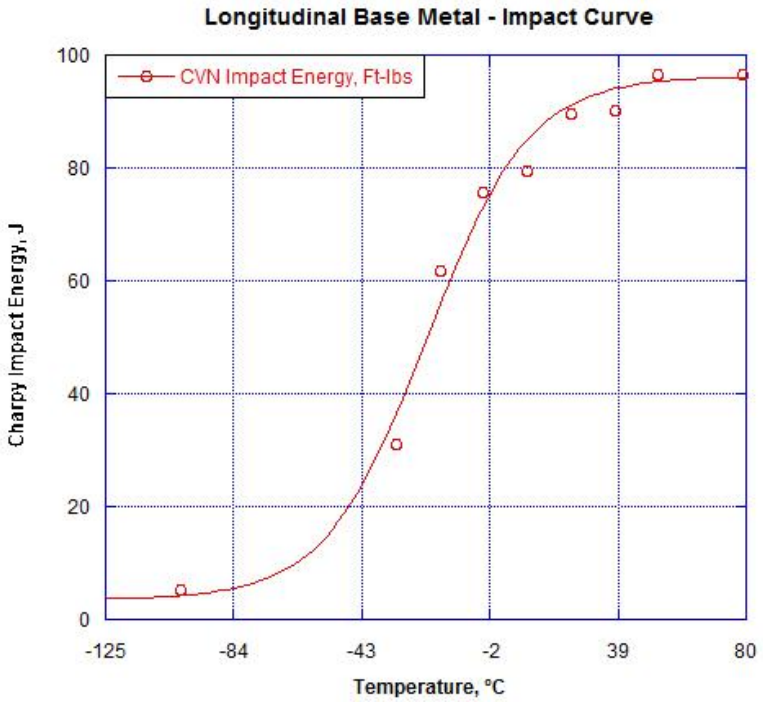

Figure 60. Charpy V-notch impact energy as a function of temperature for axial base metal samples removed from the pipe section.

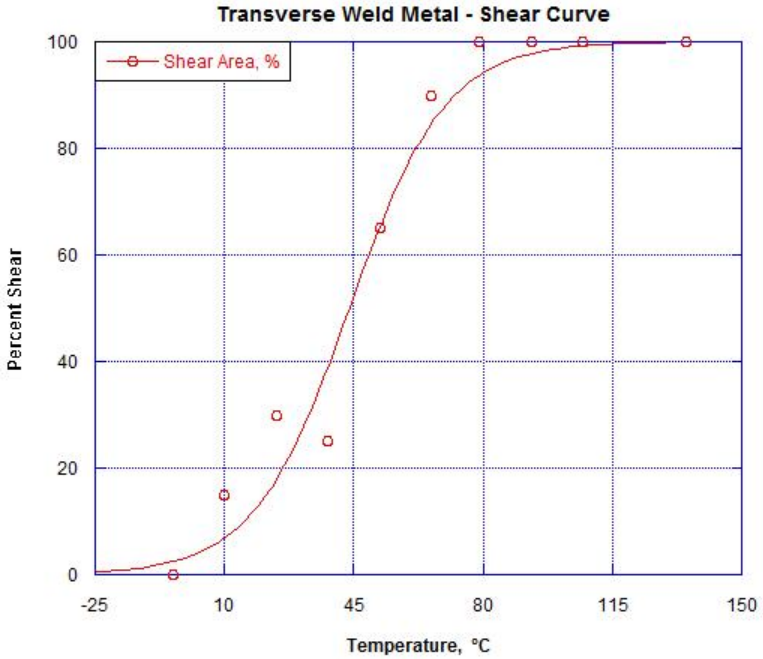

Figure 61. Percent shear from Charpy V-notch tests as a function of temperature for transverse seam weld samples removed from the pipe section.

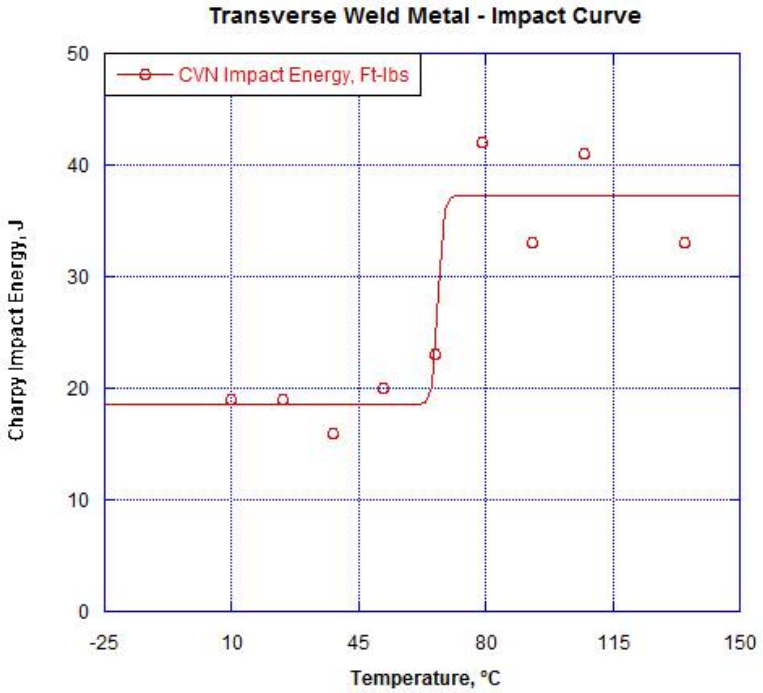

Figure 62. Charpy V-notch impact energy as a function of temperature for transverse seam weld samples removed from the pipe section.

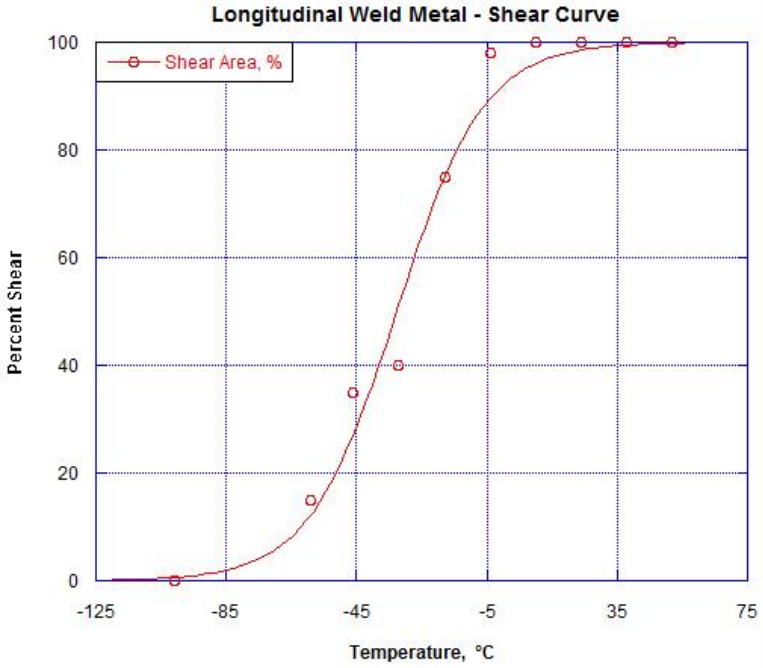

Figure 63. Percent shear from Charpy V-notch tests as a function of temperature for longitudinal seam weld samples removed from the pipe section.

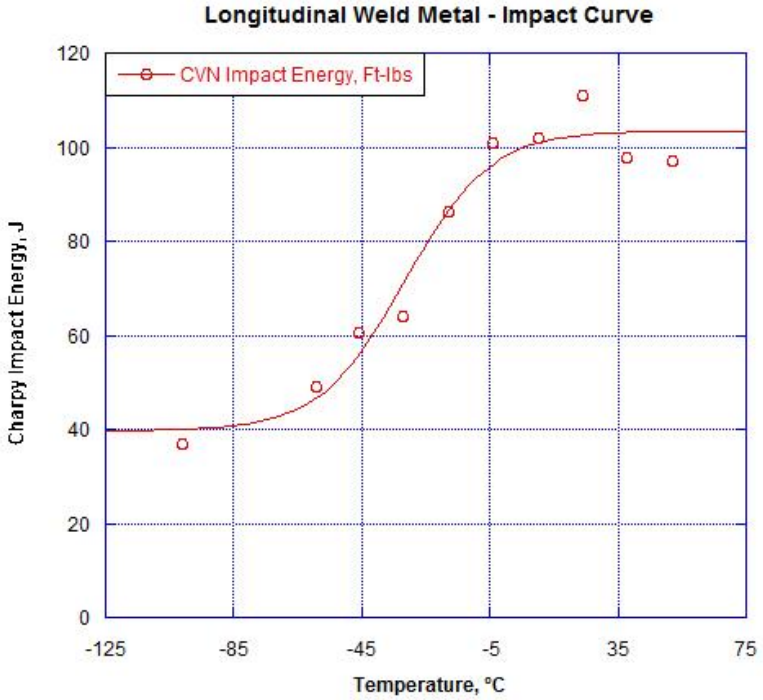

Figure 64. Charpy V-notch impact energy as a function of temperature for longitudinal seam weld samples removed from the pipe section.

Det Norske Veritas

Det Norske Veritas (DNV) is a leading, independent provider of services for managing risk with a global presence and a network of 300 offices in 100 different countries. DNV's objective is to safeguard life, property and the environment.

DNV assists its customers in managing risk by providing three categories of service: classification, certification, and consultancy. Since establishment as an independent foundation in 1864, DNV has become an internationally recognized provider of technical and managerial consultancy services and one of the world's leading classification societies. This means continuously developing new approaches to health, safety, quality, and environmental management, so businesses can run smoothly in a world full of surprises.

Global Impact for a Safe and Sustainable Future

Learn more on www.dnv.com